Importin α5 Regulates Anxiety through MeCP2 and Sphingosine Kinase 1

Nicolas Panayotis, Anton Sheinin, Shachar y Dagan, Michael M Tsoory, Franziska Rother, Mayur Vadhvani, Anna Meshcheriakova, Sandip Koley, Letizia Marvaldi, Didi-Andreas Song, et al.

Article

Cell Reports

Importin α5 Regulates Anxiety through MeCP2 and Sphingosine Kinase 1

Graphical Abstract

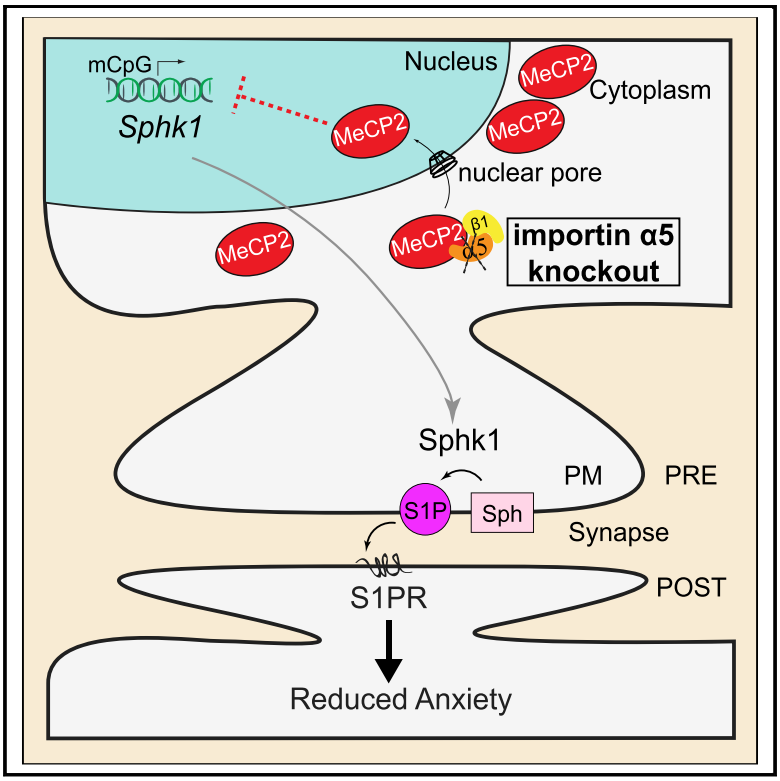

Highlights

- Reduced expression of importin α5 in hippocampal neurons decreases anxiety
- Importin α5 is required for nuclear localization of MeCP2 in hippocampal neurons
- Importin α5 knockout increases expression of Sphk1, an MeCP2-regulated gene
- Pharmacological modulation of Sphk1 and the S1P receptor affects anxiety

Authors

Nicolas Panayotis, Anton Sheinin, Shachar Y. Dagan, ..., Michael Bader, Izhak Michaelevski, Mike Fainzilber

Correspondence

mike.fainzilber@weizmann.ac.il

In Brief

Panayotis et al. found decreased anxiety in importin α5 knockout mice. They report that importin α5 influences sphingosine-sensitive anxiety pathways by regulating MeCP2 nuclear import in hippocampal neurons.

Panayotis et al., 2018, Cell Reports *25*, 3169–3179
December 11, 2018
https://doi.org/10.1016/j.celrep.2018.11.066

CellPress

Cell Reports
Article

Importin α5 Regulates Anxiety through MeCP2 and Sphingosine Kinase 1

Nicolas Panayotis,[1] Anton Sheinin,[2] Shachar Y. Dagan,[1] Michael M. Tsoory,[3] Franziska Rother,[4,5] Mayur Vadhvani,[6] Anna Meshcheriakova,[1] Sandip Koley,[1] Letizia Marvaldi,[1] Didi-Andreas Song,[1] Eitan Reuveny,[1] Britta J. Eickholt,[6] Enno Hartmann,[4,5] Michael Bader,[4,5] Izhak Michaelevski,[7] and Mike Fainzilber[1,8,*]

[1]Department of Biomolecular Sciences, Weizmann Institute of Science, Rehovot 76100, Israel
[2]Sagol School of Neuroscience, Tel Aviv University, Tel Aviv 69978, Israel
[3]Department of Veterinary Resources, Weizmann Institute of Science, Rehovot 76100, Israel
[4]Max-Delbrück-Center for Molecular Medicine, 13125 Berlin, Germany
[5]Center for Structural and Cellular Biology in Medicine, Institute of Biology, University of Lübeck, 23538 Lübeck, Germany
[6]Institute of Biochemistry, Charité-Universitätsmedizin Berlin, 10117 Berlin, Germany
[7]Department of Molecular Biology, Integrative Brain Research Center - Ariel, Ariel University, Ariel 40700, Israel
[8]Lead Contact
*Correspondence: mike.fainzilber@weizmann.ac.il
https://doi.org/10.1016/j.celrep.2018.11.066

SUMMARY

Importins mediate transport from synapse to soma and from cytoplasm to nucleus, suggesting that perturbation of importin-dependent pathways should have significant neuronal consequences. A behavioral screen on five importin α knockout lines revealed that reduced expression of importin α5 (KPNA1) in hippocampal neurons specifically decreases anxiety in mice. Re-expression of importin α5 in ventral hippocampus of knockout animals increased anxiety behaviors to wild-type levels. Hippocampal neurons lacking importin α5 reveal changes in presynaptic plasticity and modified expression of MeCP2-regulated genes, including sphingosine kinase 1 (Sphk1). Knockout of importin α5, but not importin α3 or α4, reduces MeCP2 nuclear localization in hippocampal neurons. A Sphk1 blocker reverses anxiolysis in the importin α5 knockout mouse, while pharmacological activation of sphingosine signaling has robust anxiolytic effects in wild-type animals. Thus, importin α5 influences sphingosine-sensitive anxiety pathways by regulating MeCP2 nuclear import in hippocampal neurons.

INTRODUCTION

Anxiety and stress-related conditions are a significant health burden in modern society. Pharmacological interventions have implicated several hormones and neurotransmitters in anxiety modulation (Dias et al., 2013; Griebel and Holmes, 2013), but intracellular transport systems have not been studied in this context. Coupling neurotransmitter signals to behavioral output likely requires changes in transcription in neurons (West and Greenberg, 2011), necessitating information transfer from synapse to nucleus (Herbst and Martin, 2017; Lim et al., 2017; Saito and Cavalli, 2016). Members of the importin family of nuclear import factors have pivotal roles in such pathways because of their involvement in intracellular transport between synapse and soma (Panayotis et al., 2015) and between cytoplasm and nucleus (Miyamoto et al., 2016). However, importins and related molecules have not been studied for potential roles in anxiety regulation to date.

Nuclear import factors from the importin α subfamily directly bind nuclear localization signals (NLSs) in cargo proteins in cooperation with importin β1. There are 6–7 importin α family members in any given mammal (Table S1), and individual cell types express different subsets of this ensemble (Pumroy and Cingolani, 2015), often in a tightly regulated manner (Yasuhara et al., 2007, 2013). Injury in peripheral neurons (Ben-Yaakov et al., 2012; Hanz et al., 2003; Perry et al., 2012; Terenzio et al., 2018; Yudin et al., 2008) or activity in central neurons (Ch'ng et al., 2012; Dieterich et al., 2008; Jeffrey et al., 2009; Karpova et al., 2013; Thompson et al., 2004) can activate importin-dependent transport mechanisms in axons or dendrites to link both pre- and postsynaptic compartments to soma and nucleus (Lim et al., 2017; Rishal and Fainzilber, 2014). Assigning specific roles for individual importin α's in brain functions is challenging due to functional redundancies in cargo binding (Friedrich et al., 2006; Ushijima et al., 2005) and compensatory expression regulation of different family members (Shmidt et al., 2007). We addressed this issue by subjecting five importin α knockout (KO) mouse lines to a comprehensive battery of behavioral tests. Of the five lines analyzed, comprising single-gene knockouts for importin α1, α3, α4, α5, and α7 (Gabriel et al., 2011; Rother et al., 2011; Shmidt et al., 2007), the importin α5 knockout was the only line to reveal significantly reduced anxiety phenotypes. The molecular mechanism underlying importin α5-dependent anxiolysis is elucidated here.

RESULTS

An Anxiolytic Phenotype in Importin α5 Knockout Mice

Behavioral phenotyping was performed on five single-gene importin α knockout mouse lines, all of which were viable and reached adulthood. We used a panel of assays to follow

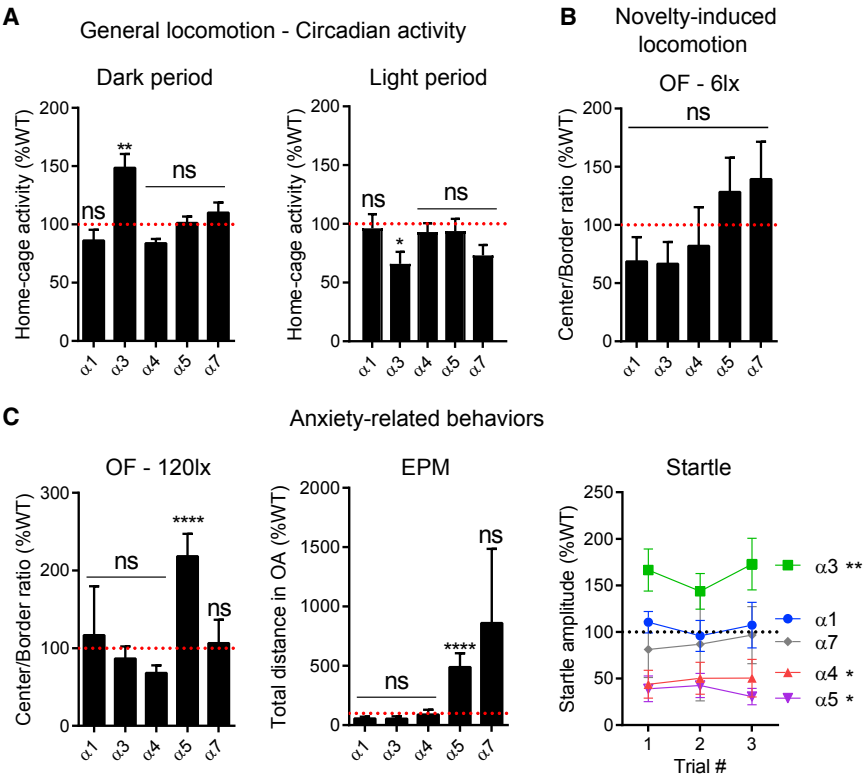

Figure 1. Behavioral Phenotyping of Different Importin α Knockout Mice

The tests used cover (A) general locomotion and circadian activity, (B) novelty-induced locomotion, and (C) anxiety-related behaviors.

(A) Basal home-cage activity of the mice in a home-cage locomotion test. An InfraMot system was used to monitor the activity of the mice over 72 consecutive hours. Most importin α-knockout mouse lines do not exhibit significant modification of their activity during dark or light periods (α1, α4, α5, and α7; $p > 0.05$). Importin α3 knockouts showed elevated activity compared to wild-type during the dark phase (148% ± 11.9%; $p < 0.05$) and decreased activity during the light phase (66.03% ± 10.17%; $p < 0.05$).

(B) Novelty-induced locomotion was assessed in an open-field test performed under dim light (open-field-6 lux). No significant differences were observed for all importin α mutants compared to their wild-type littermates.

(C) Anxiety measures from the open-field test (OF-120 lux) show an increased center-to-border ratio for importin α5 null mice. In the elevated plus maze, importin α5 mice travelled more in the open (i.e., unsecured and anxiogenic) arms. Importin α5 null mice displayed a decreased baseline acoustic startle, in accordance with a reduction in anxiety-related behaviors in this line. Importin α3 results indicate an increased startle response, and importin α4 nulls present a deficit in the startle response.

8–15 animals were used for each line in the different assays of this dataset. *$p < 0.05$, **$p < 0.01$, ***$p < 0.001$, ****$p < 0.0001$; two-tailed t test. All data error bars represent mean ± SEM. See also Data S1.

home-cage locomotion and circadian activity, novelty-induced locomotion, and anxiety behaviors (Figure 1; Data S1). Importin α5 knockout animals displayed a specific phenotype characterized by reduced anxiety in multiple tests, including open field, elevated plus maze, and acoustic startle response. Open-field and elevated plus maze tests are based on the monitoring of mouse locomotion activity when placed in a novel environment offering both secure and anxiogenic areas (Prut and Belzung, 2003; Walf and Frye, 2007). In contrast, the acoustic startle response monitors a reflex-based response to a sudden loud sound (Koch, 1999). Importin α5 knockout mice explored and reared significantly more than their wild-type littermates in the central anxiogenic area of the open field (Figures 2A–2C). The specificity of the result was confirmed by the absence of effects on total distance traveled or velocity of movement, as well as time spent in the open-field anxiogenic area under low illumination (6 lux, assessing general motor activity) (Trullas and Skolnick, 1993), ruling out possible general movement phenotypes in these mice (Figure S1A).

In line with the open-field results, importin α5 knockout mice showed a significant increase in distance covered, time spent, and number of visits in the open arms of the elevated plus maze compared to their wild-type littermates (Figures 2D–2F; Figure S1B). We examined their anxiety responses in an acoustic startle response test, monitoring the involuntary motor reflex to a loud auditory stimulation of 120 dB. Importin α5 knockout mice exhibited both a significant increase in reaction time and a significantly reduced response amplitude compared to wild-type littermates (Figures 2G–2I). The importin α5 knockout was the only line of the five importin α mutants tested that revealed a consistent phenotype in all three anxiety tests, emphasizing the robustness of the findings. Moreover, importin α5 knockout animals did not reveal differences in home-cage activity or performance in rotarod, wire hanging, and pole tests (Figures S1C–S1F). Learning and memory features of the importin α5 knockouts were assessed in Morris water maze (MWM) setups (Figures S1G–S1M). Although there was an apparent lower performance of the importin α5 knockout animals, the reduction in time spent scanning for the escape platform (Figure S1J) was not compensated by more sustained exploration of the other quadrants (Figure S1K). Hence, these MWM data may also reflect lower anxiety of the importin α5 knockouts, with less urgency to escape the MWM than their wild-type counterparts. Altogether, this battery of additional assays supports a specific reduction in anxiety levels in importin α5 null mice, without changes in other physiological parameters of overall motor performance, coordination, or activity.

Anxiety-related responses are influenced by changes in synaptic plasticity, which are reflected in abnormal responses in the hippocampus or the amygdala (Bannerman et al., 2014; Jimenez et al., 2018; Tovote et al., 2015). We therefore assessed basal synaptic transmission, presynaptic-dependent short-term plasticity,

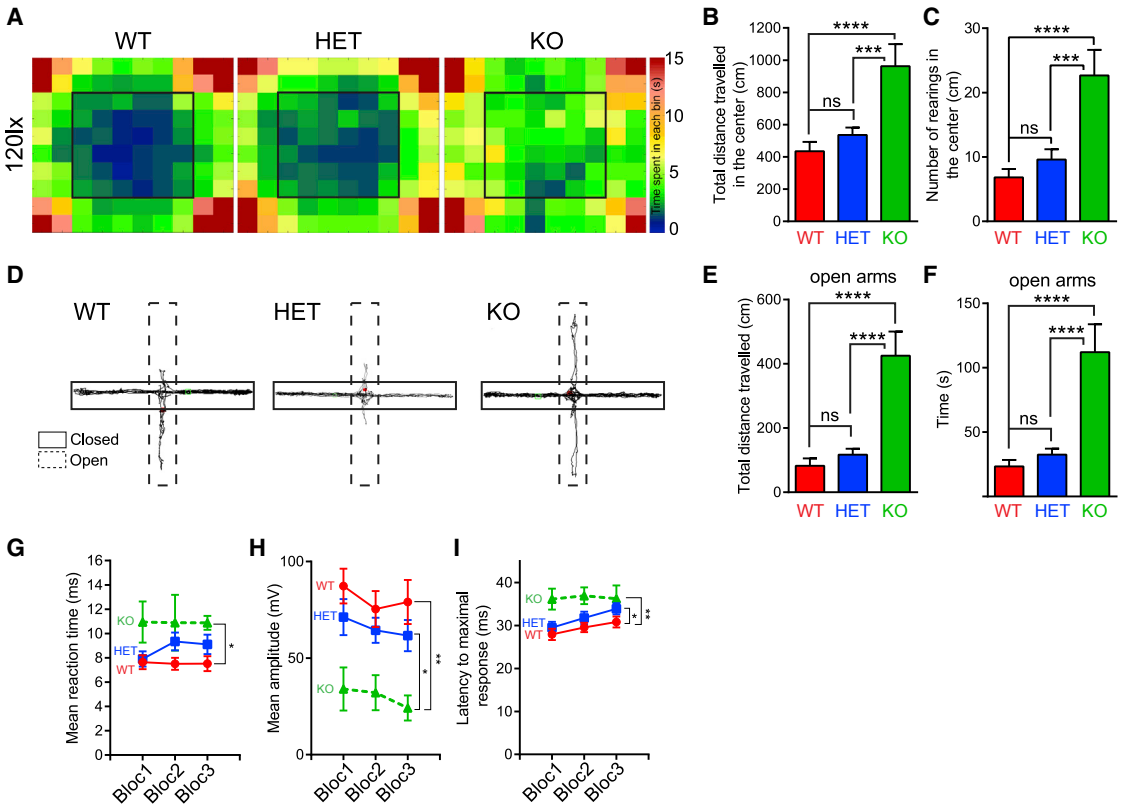

Figure 2. Reduced Anxiety in Importin α5 Knockout Mice

(A–C) Group heatmap representation (A) of mouse activity over 10 min in the open field. Importin α5 knockout mice exhibit significant increases in the time spent, the distance traveled (B), and rearing activity (C) in the open-field center.

(D–F) Importin α5 knockout mice show increased exploration of the open arms of an elevated plus maze, as shown by representative track traces (D), significantly higher distance coverage (E), and time spent (F) in the open arms compared to wild-type littermates.

(G–I) Results from an acoustic startle response test monitoring the motor reflex to 120 dB auditory stimulation. Importin α5 knockout mice revealed a significant increase in reaction time (G) to the auditory stimulus ($p < 0.05$), a significant decrease in response amplitude (H), and a delay of the peak response (I) compared to wild-type littermates.

$n \geq 9$ animals for each genotype per test. *$p < 0.05$, **$p < 0.01$, ***$p < 0.001$, ****$p < 0.0001$; one-way ANOVA followed by Tukey's HSD post hoc correction for multiple comparisons. All data error bars represent mean ± SEM. See also Figure S1.

and long-term potentiation (LTP) at hippocampal Schaffer collateral synapses (Figure 3; Figure S2). The most prominent effects were observed in short-term synaptic plasticity associated with paired-pulse facilitation (PPF) or paired-pulse depression (PPD), revealing marked depression in importin α5 knockout slices, in contrast to facilitation in wild-type, at all time points measured. Overall, the data indicate a presynaptic deficit in importin α5 knockout hippocampus, suggesting differential regulation of synaptic vesicle pools and presynaptic calcium levels and distribution in the mutant mice. Moreover, analysis of basal synaptic transmission revealed stronger excitability patterns in knockout and heterozygous mice versus wild-type, although the magnitude of the field excitatory postsynaptic potential (fEPSP) slope at maximal stimulation intensity was similar in all tested groups.

A Transcriptional Component in Importin α5-Dependent Anxiolysis

We used the anxiogenic drug FG-7142 (Evans and Lowry, 2007) to test whether the reduction in anxiety in importin α5 knockout mice is amenable to pharmacological modulation. FG-7142 increases anxiety by a partial agonist effect on the γ-aminobutyric acid A (GABA-A) receptor (Figure 4A) and hence provides a convenient tool to test whether anxiolysis in importin α5 knockout animals is hard wired or is reversible (Figure 4B). FG-7142 reversed anxiolysis in importin α5 knockout animals in open-field tests without affecting overall movement velocity in the test (Figures 4C–4F). We then proceeded to analyze hippocampal transcriptomes by RNA sequencing (RNA-seq). RNA was extracted from total hippocampi, which were dissected from either importin α5 or wild-type (WT) animals injected with vehicle or FG-7142. Analyses of the resulting datasets revealed significant changes in the expression of 121 genes under basal conditions in importin α5 null mice (Figures 5A and 5B) and a larger cohort of almost 600 transcripts that were differentially regulated by FG-7142 treatment in knockout versus wild-type mice (Figures S3A and S3B; Table S2). We then performed computational analyses of these differential groups to reveal the underlying transcriptional networks, using the TRANSFAC

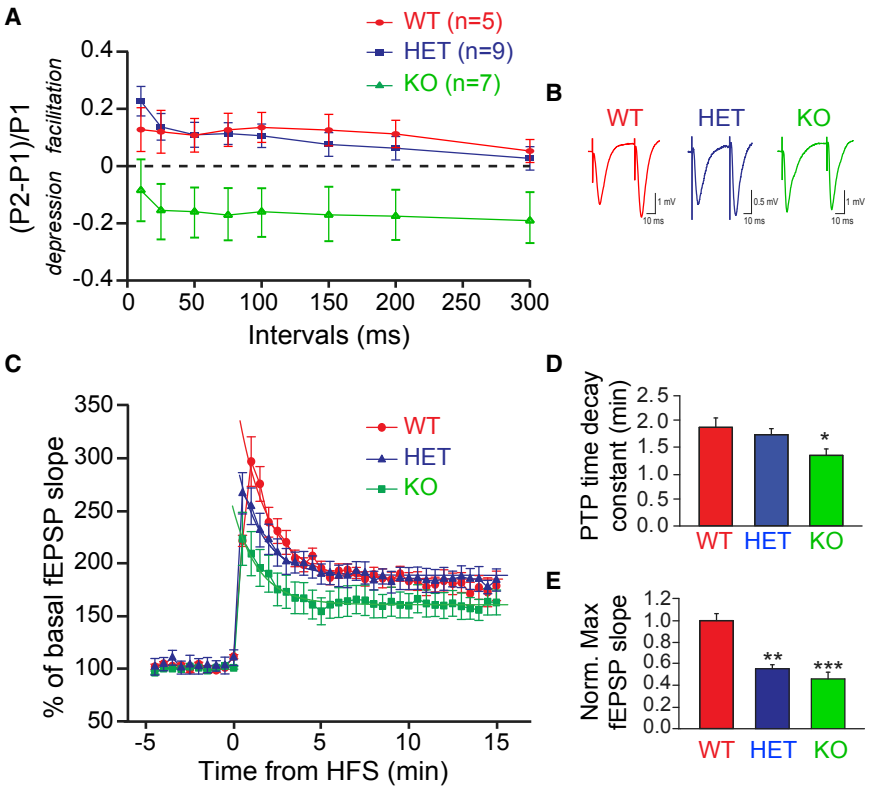

Figure 3. Synaptic Effects of the Importin α5 Knockout

(A) Dependence of paired-pulse facilitation or depression on the interval between two presynaptic stimulations in hippocampal slice preparations. The paired-pulse facilitation or depression is determined as a normalized increase or decrease in the amplitude of the second fEPSP, according to the following equation: $(P2 - P1)/P1$, where P1 and P2 are the amplitudes of the first and second fEPSPs, respectively. In contrast to wild-type or heterozygous mice, knockout slices revealed marked depression in response to the paired-pulse protocol at all measured time points.

(B) Raw data examples of paired fEPSP responses acquired at presynaptic stimulation interval of 50 ms from hippocampal slices from all three genotypes (stimulation [stim], CA3; recording, CA1).

(C) Post-tetanic potentiation (PTP) estimated as an immediate increase of fEPSP slope after high-frequency stimulation (HFS).

(D) The PTP decay time constant was found to be significantly lower in α5 knockout mice. PTP The decay time constant was derived using the exponential decay function: $fEPSP - slope = fEPSP - slope - max * e^{(t/\tau)} + const.$, where t is a time of fEPSP recording and τ is the fEPSP decay time constant, representing the PTP decay time constant. The equation was used to fit the normalized to the baseline fEPSP slopes shown in (C).

(E) Normalized maximal fEPSP slope showing PTP magnitude was lowest in α5 knockout mice. Normalized maximal fEPSP slope was derived from the exponential decay fit equation described in (D).

n = 5 WT (wild-type), 9 HET (heterozygous), and 7 knockout (α5 knockout) in each test. *p < 0.05, **p < 0.01, ***p < 0.001; one-way ANOVA with Holm-Sidak post hoc analysis. See also Figure S2.

FMatch promoter analysis tool, and the enriched pathways and signaling networks, using the Ingenuity tool (Figure S3C). The resulting list of transcription factors (TFs) that may control expression of importin α5 knockout differentially expressed genes (DEGs) features several interesting candidates, most prominently MeCP2 (Figure 5C), a transcriptional modulator best known as the gene mutated in Rett syndrome (Lyst and Bird, 2015). MeCP2 gene dosage is known to affect anxiety behaviors (Goffin et al., 2011; Na et al., 2012; Samaco et al., 2012; Stearns et al., 2007). The Ingenuity pathway analyses (Figures S3C and S3D) directed our attention to a lipid signaling network containing sphingosine kinase 1 (Sphk1), an MeCP2-regulated gene (Figure 5C). The upregulation of Sphk1 in importin α5 knockout hippocampus is intriguing, because previous studies have implicated Sphk1, its product sphingosine 1 phosphate (S1P), and its receptors in synaptic plasticity and presynaptic functions (Chan and Sieburth, 2012; Kanno et al., 2010; Kempf et al., 2014).

Importin α5 Is Required for MeCP2 Nuclear Localization in Hippocampal Neurons

Multiple nuclear import routes have been described for MeCP2 (Baker et al., 2015; Lyst et al., 2018); hence, we first assessed MeCP2 interaction with importin α5 by fluorescence resonance energy transfer (FRET) acceptor photobleaching. A significant FRET signal was revealed in human embryonic kidney (HEK) cells cotransfected with MeCP2-GFP and importin α5-mScarlet (Figures 5D and 5G), while no such signal was observed when MeCP2-GFP was substituted by cytosolic GFP or phosphotriesterase (PTE)-GFP constructs (Figures 5E–5G). We then performed a series of immunofluorescence analyses to assess MeCP2 expression and nuclear localization in the dorsal hippocampus (dHPC), the ventral hippocampus (vHPC), the amygdala, and the motor cortex, comparing importin α5 knockouts and their wild-type littermates. As shown in Figure 5H, MeCP2 localization was strictly nuclear and highly colocalized with DAPI-positive heterochromatin in wild-type ventral hippocampus neurons (90% colocalization) and ranged above 72% in all other brain areas tested (Figure 5I; Figures S4A and S4B). In contrast, importin α5 knockout brains revealed significant and specific exclusion of MeCP2 from the nuclei of both ventral hippocampus and dorsal hippocampus neurons (Figures 5H and 5I), but not in amygdala or motor cortex (Figure 5I; Figures S4A and S4B). There were no deficits in MeCP2 nuclear localization in all brain regions examined from importin α3 and importin α4 knockout mice (Figures S4C–S4F).

To validate these findings by another approach, we evaluated MeCP2 nuclear levels by western blot analyses of purified nuclear fractions from ventral hippocampus and amygdala, focusing on these regions due to their key roles in anxiety circuits (Bannerman et al., 2014; Jimenez et al., 2018; Tovote et al.,

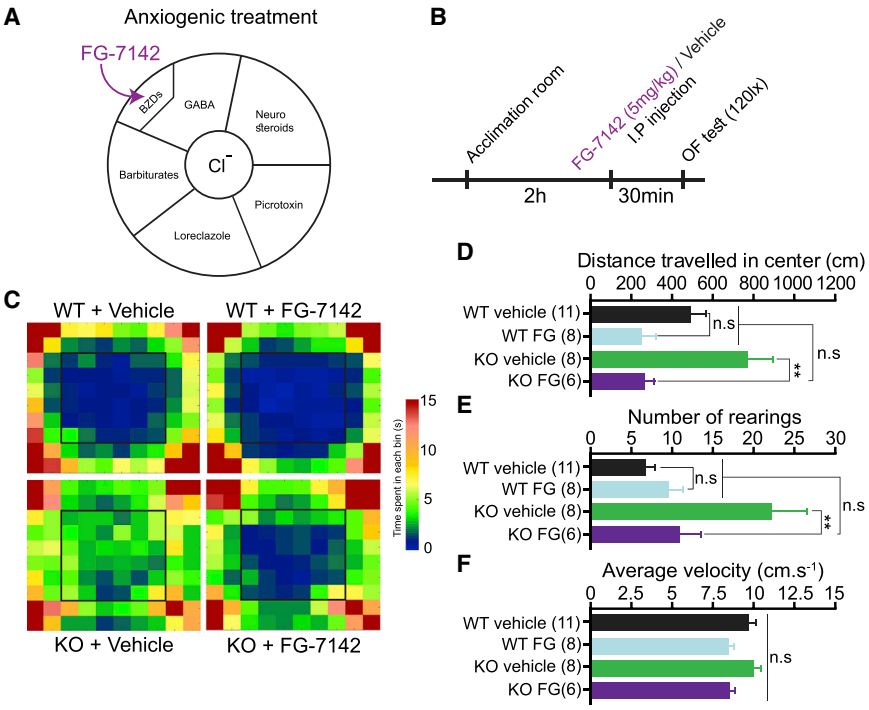

Figure 4. Effects of the Anxiogenic Drug FG-7142 on Wild-Type and Importin α5 Knockout Mice

(A) Schematic of the GABA-A receptor showing the benzodiazepine binding site where FG-7142 acts as an inverse partial agonist.

(B) FG-7142 (5 mg/kg) or vehicle was injected intraperitoneally, and its effects were assessed in an open field after 30 min.

(C) Open-field activity heatmaps show that the anxiolytic phenotype of importin α5 knockout mice is reversed by FG-7142 treatment.

(D–F) FG-7142 treatment significantly decreases the distance traveled in the center of the open field (D) and the number of rearing events in the center (E) but did not perturb the average movement velocity (F).

The number of animals per group is indicated in parentheses. *$p < 0.05$, **$p < 0.01$, ***$p < 0.001$; one-way ANOVA followed by Tukey's HSD post hoc correction for multiple comparisons (D–F). All data error bars represent mean ± SEM.

2015). The analysis revealed a significant reduction of MeCP2 levels in nuclear extracts of importin α5 knockout ventral hippocampus, but not amygdala (Figures 5J and 5K). There were no significant differences in MeCP2 levels in nuclear extracts from either brain region from importin α3 or α4 mice (Figures 5J and 5K), consistent with the immunofluorescence analyses described earlier. Thus, importin α5 is critical for MeCP2 nuclear localization in the ventral and dorsal hippocampus. The lack of effect of single-gene importin knockouts in amygdala and motor cortex may reflect different nuclear import routes for MeCP2 in those neuronal subtypes.

Adult Ventral Hippocampus Importin α5 Knockdown Reduces Anxiety Behaviors

We examined the role of importin α5 gene dosage in the ventral hippocampus for anxiety behavior using virus-driven knockdown by stereotaxic injection (Figures S5A and S5B). A short hairpin RNA (shRNA) targeting murine importin α5 (shα5) was validated for importin α5 knockdown *in vivo*, compared with a shRNA scrambled sequence control (sh-scramble) (Figure S5C). Three weeks after bilateral ventral hippocampus stereotaxic injection of shα5 or sh-scramble, mice were evaluated in open-field (OF), elevated plus maze (EPM), fear conditioning, and startle response tests. Mice injected with either lentiviral or adeno-associated virus serotype 5 (AAV5)-expressing shα5 showed reduced anxiety in the open-field (Figures 6A–6D and 6H–6K) and the elevated plus maze (Figures 6E–6G and 6L–6N) tests compared to the corresponding sh-scramble controls. The ventral hippocampus-injected importin α5 knockdown (KD) mice did not show alteration in fear conditioning freezing or startle responses (Figures S5D and S5E), suggesting no significant alterations in amygdala-dependent fear memory or in pathways associated with acoustic startle (Tovote et al., 2015). We then sought to revert anxiety attenuation in importin α5 knockdown mice by concomitant expression of an shα5-resistant human importin α5 expression construct. Importin α5 levels were preserved upon coinjection of the human expression construct, together with shα5 (Figure S5C), and anxiety-related behaviors did not differ between coinjected mice and sh-scramble controls (Figures 6H–6N). Hence, acute and specific knockdown in the adult ventral hippocampus confirms a role for hippocampal importin α5 in regulation of anxiety.

Pharmacological Targeting of the Importin α5 Anxiolysis Pathway

The data summarized earlier suggest that importin α5 regulates anxiety through MeCP2 and sphingosine signaling pathways (Figure 7A). Tissue-dependent expression of Sphk1 is controlled by DNA methylation-dependent repression (Imamura et al., 2004), and MeCP2 gene dosage can influence Sphk1 in the mouse brain (Gabel et al., 2015). Removal of importin α5 reduces MeCP2 levels in the nucleus, thereby enabling increased expression of Sphk1, followed by enhanced activation of S1P receptors. This model predicts that S1P receptor agonists should have anxiolytic effects, while Sphk1 antagonists should be anxiogenic. Moreover, an effective Sphk1 antagonist should attenuate the anxiolytic phenotype in importin α5 knockout mice. We therefore tested the effects of two such molecules: fingolimod, an S1P receptor agonist used as a drug in multiple sclerosis (Chew et al., 2016), and PF-543, a selective inhibitor of Sphk1 (Schnute et al., 2012).

We tested the effects of the S1P receptor agonist fingolimod using a dose regime previously employed for trophic factor studies in the hippocampus (Deogracias et al., 2012). Fingolimod markedly reduced anxiety levels in both elevated plus maze

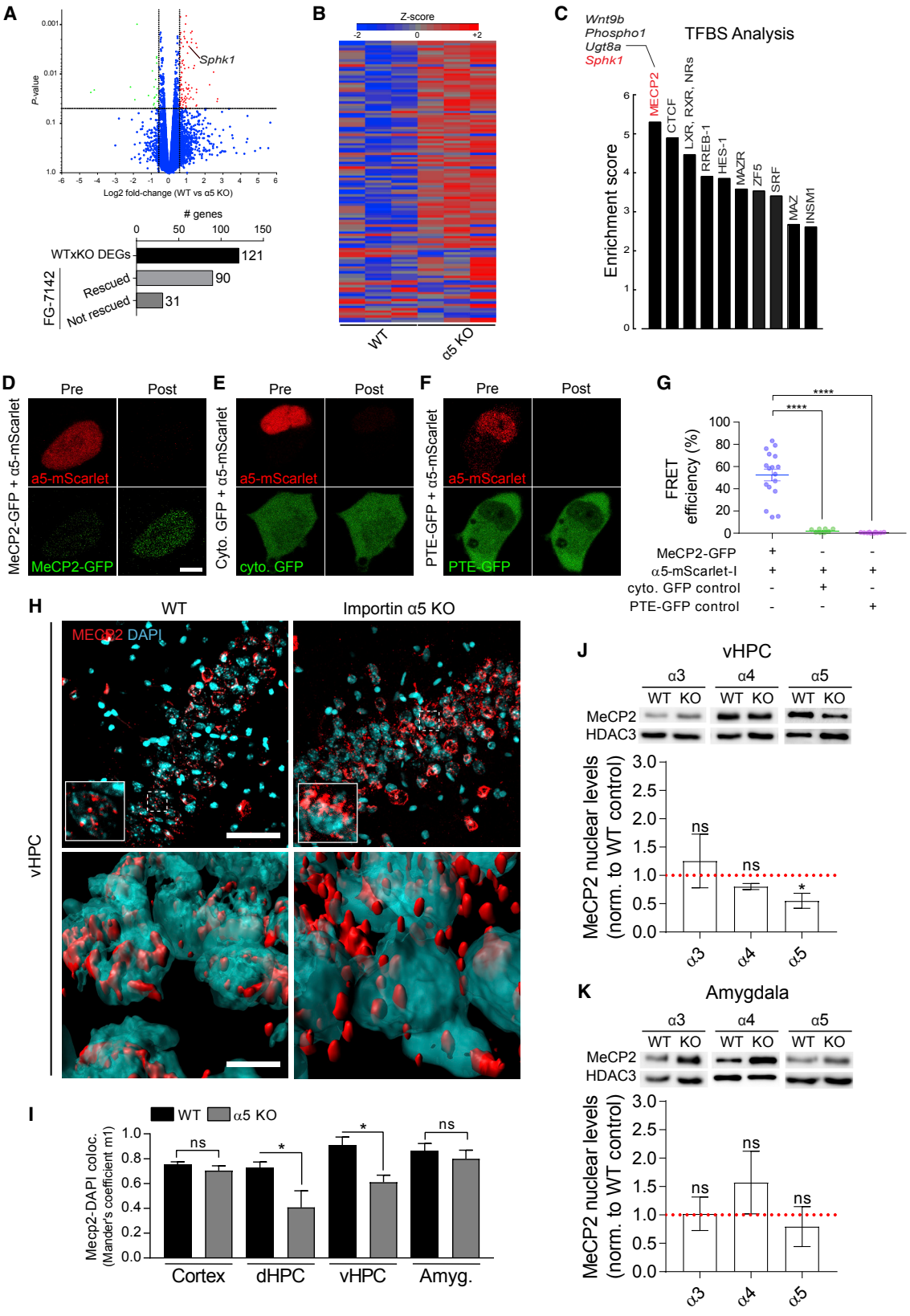

(legend on next page)

(Figures 7B–7D) and open-field assays (Figures S6A–S6C). We repeated these assays on BALB/c mice, a line with intrinsically higher anxiety levels than the C57BL/6 mice used thus far throughout our study (Oliverio et al., 1973). Most strikingly, BALB/c mice likewise exhibited significantly reduced anxiety responses upon fingolimod treatment, despite their clearly apparent higher basal anxiety measures (Figures 7E–7G; Figures S6D–S6F). Finally, we tested the effects of the Sphk1 inhibitor PF-543 by intraperitoneal (i.p.) injection in wild-type and importin α5 knockout animals. Sphk1 inhibition did not influence anxiety-related behavior of wild-type mice in the elevated plus maze. However, it significantly decreased the distance traveled and the time spent in the open arms for importin α5 knockout animals (Figures 7H–7J). Hence, Sphk1 inhibition reverses the anxiety reduction phenotype of importin α5 knockout mice as predicted.

DISCUSSION

Our findings highlight roles for importin α5 and MeCP2 in anxiety regulation. Previous studies (Shmidt et al., 2007) and our own analyses demonstrated normal brain development and a lack of other behavioral abnormalities in the importin α5 knockout mouse, emphasizing the specificity of the anxiety phenotype. This specificity is most likely due to the requirement for importin α5 for nuclear import of MeCP2 in certain neuronal subtypes, including in the hippocampus. Patients suffering from Rett syndrome or from MeCP2 duplication syndrome present with anxiety disorders as part of the clinical spectrum (Barnes et al., 2015; Ramocki et al., 2009), and anxiety phenotypes have been described for various MeCP2 mutant mouse models (Goffin et al., 2011; Na et al., 2012; Samaco et al., 2008; Stearns et al., 2007). Our data suggest that targeting importin α5 to reduce MeCP2 nuclear import can attenuate anxiety, and it will be interesting to test whether targeting importin α5 might ameliorate other aspects of MeCP2-related diseases in the future.

The findings implicate the sphingosine signaling pathway in importin α5/MeCP2-dependent anxiety regulation. Several studies have linked sphingolipids to anxiety disorders, but the mechanisms involved are not fully understood (Mühle et al., 2013; Müller et al., 2015). We provide both molecular and pharmacological evidence for the involvement of Sphk1 and S1P in anxiety pathways. The clear anxiolytic effects of fingolimod suggest that this pathway provides new targets for anxiety drug development and demonstrate the possibility of repurposing existing drugs to anxiety therapy. In this context, a prospective study described a decrease in anxiety levels in multiple sclerosis patients upon initiation of fingolimod treatment (Moreau et al., 2017). Current therapies for anxiety disorders either directly affect neurotransmitter receptor systems or modulate neurotransmitter levels or availability, but their long-term use is limited by problematic side effects and suboptimal efficacy (Griebel and Holmes, 2013). Despite keen interest in the development of mechanistically novel anxiolytic drugs, these have not been forthcoming over the past two decades (Murrough et al., 2015). We hope that the anxiety-regulating mechanisms identified here may provide new avenues to this end.

STAR★METHODS

Detailed methods are provided in the online version of this paper and include the following:

- KEY RESOURCES TABLE
- CONTACT FOR REAGENT AND RESOURCES SHARING
- EXPERIMENTAL MODEL AND SUBJECT DETAILS
  - Animal Subjects
- METHOD DETAILS
  - Pharmacological treatments
  - Hippocampal slice preparation
  - Electrophysiology
  - Lentiviral and AAVs vector design and production
  - Intracerebral injections of lentiviral vectors and AAVs
  - RNA expression analysis (RNA-Seq)
  - Library Construction and Sequencing
  - Sequence Data/ Bioinformatics Analysis
  - Gene expression analysis by RT-qPCR
  - Transcription Factor Binding Site (TFBS) analysis
  - Immunofluorescence

Figure 5. Transcriptional Effects of the Importin α5 Knockout Reveal a Specific Role for MeCP2

(A) Volcano plot illustrating the gene expression results (top panel) and bar graph (bottom panel) showing the number of deregulated genes (fold change > 1.5) in α5 knockout hippocampus and the ratio of genes for which the levels of expression were rescued or not under an anxiogenic treatment (5 mg/kg FG-7142).

(B) Heatmap representation of *Z* score-transformed normalized expression values for 121 genes with significantly changed expression in importin α5 knockout hippocampus (n = 3 mice per group).

(C) Top 10 transcription factor candidates identified by an FMatch (geneXplain) search for factors regulating expression of genes differentially expressed in importin α5 knockout. Genes regulated by MeCP2 are listed in the inset.

(D–F) Confocal images of HEK cells transfected with MeCP2-GFP and importin α5-mScarlet (D), cytoplasmic-GFP and importin α5-mScarlet (E), and PTE-GFP and importin α5-mScarlet (F). The images were taken before (pre) and after (post) photobleaching of the acceptor (mScarlet) using a region of interest (ROI) delineating the cell (scale bar, 5 μm).

(G) Average FRET efficiency ± SEM (n of 9–17 cells per condition).

(H) Immunofluorescence for MECP2 (red) and DAPI nuclear staining (blue) revealed a clear punctate heterochromatic pattern in neuronal nuclei in the ventral hippocampus (vHPC; CA3 region) of wild-type mice, with reduced colocalization in importin α5 knockout (scale bar, 50 μm). The bottom panel represents the isosurface rendering of wild-type and α5 knockout nuclei (scale bar, 10 μm).

(I) Average Mander's coefficient of colocalization quantified in the motor cortex, dorsal hippocampus (dHPC), ventral hippocampus, and amygdala of wild-type versus importin α5 knockout mice (n ≥ 3 per genotype and structure).

(J and K) Immunoblots of MeCP2 and HDAC3 in nuclear extracts from the ventral hippocampus (J) and amygdala (K) of importin α3-, α4-, or α5-deficient animals and their respective wild-type littermates. Normalized MeCP2 levels are shown below the blots (each replicate consists of 2 animals per genotype and per line, n = 4–6 experimental replications).

*p < 0.05, **p < 0.01; unpaired two-tailed t test (G, I, J, and K). All data error bars represent mean ± SEM. See also Figures S3 and S4.

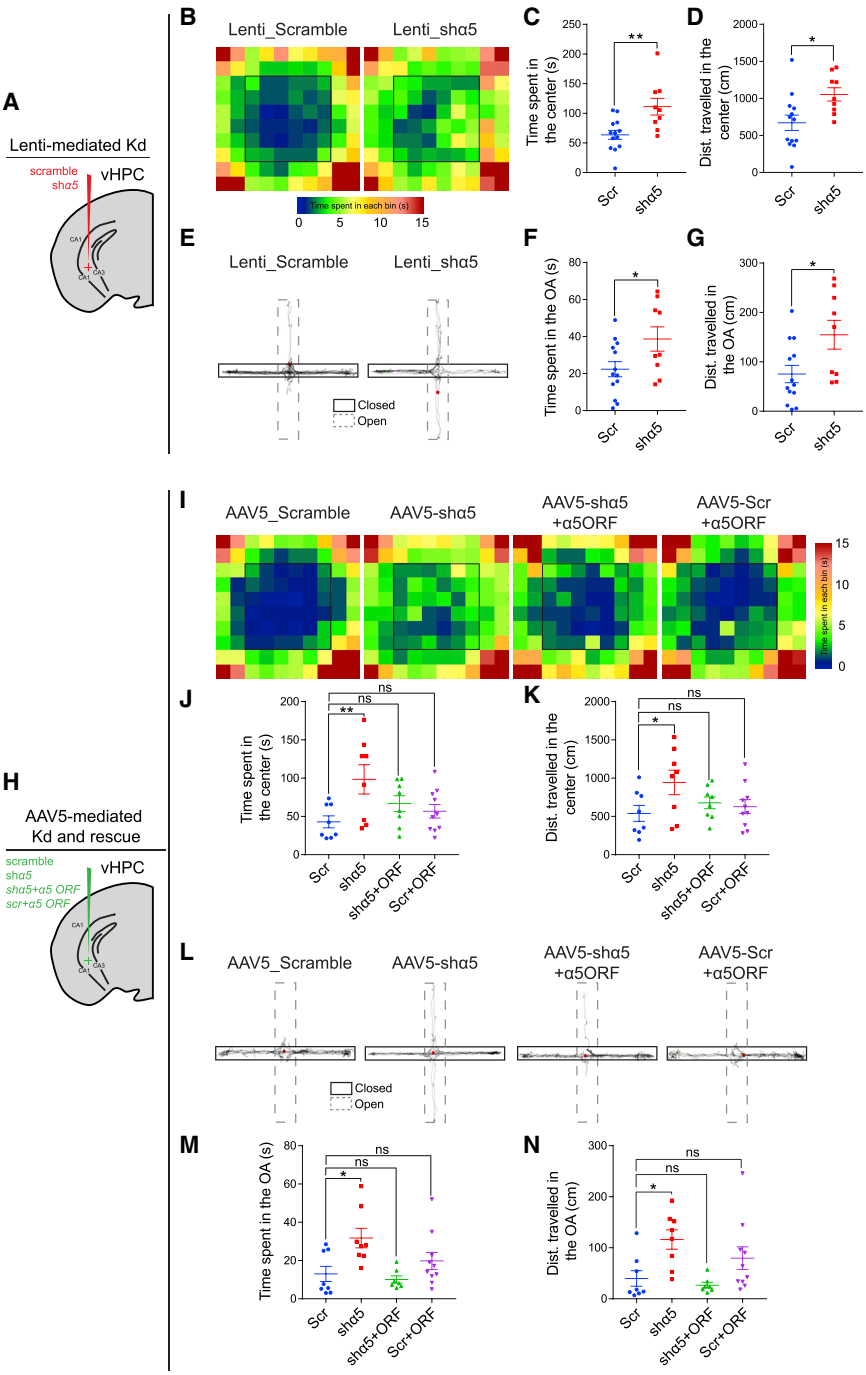

Figure 6. Acute Knockdown of Importin α5 in the Ventral Hippocampus of Adult Mice

(A) Lentiviral shRNA knockdown of importin α5 by stereotaxic injections in the ventral hippocampus.

(B–D) Ventral hippocampus-specific targeting results in the reduction of anxiety-related behaviors in the open-field test, as shown by the increased time spent ($p < 0.01$) in the center area (B and C) and the higher distance covered ($p < 0.05$) in the center (D) by shα5-injected animals compared to the scramble-injected controls.

(E–G) shα5 mice show increased exploration of the open arms of an elevated plus maze, as shown by representative track traces (E), significantly higher time spent (F), and distance coverage (G) (both $p < 0.05$) compared to their scramble-injected littermates (n = 13 Lenti_scramble, n = 9 Lenti_shα5).

(H) AAV-mediated knockdown and rescue of importin α5 expression by stereotaxic injections of shRNA alone or in combination with an importin α5-expressing rescue construct in the ventral hippocampus.

(I–K) AAV-driven knockdown of importin α5 (AAV5-shα5) in the ventral hippocampus results in the reduction of anxiety-related behaviors in the open-field test, as shown by the increased time spent ($p < 0.01$) in the center area (I and J) and the higher distance covered ($p < 0.05$) in the center (K). In contrast, the rescued mice (AAV5-shα5 + importin α5 open reading frame [α5ORF]) do not show significant differences compared to their scramble-injected littermates.

(L–N) shα5 knockdown mice show increased exploration of the open arms of an elevated plus maze, as shown by representative track traces (L), significantly higher time spent (M), and distance coverage in the open arms (N) (both $p < 0.05$). The rescued mice (AAV5-shα5 + α5ORF) did not exhibit differences compared to their scramble-injected littermates. The mice receiving both the scramble and the α5 construct (AAV5-scramble + α5ORF), were not affected in the open field or in the elevated plus maze. (n = 8 AAV5_scramble, n = 8 AAV5_shα5, n = 7–8 AAV5-shα5+α5ORF, n = 10 AAV5-scramble+α5ORF).

*$p < 0.05$, **$p < 0.01$; unpaired two-tailed t test (C, D, F, and G) and one-way ANOVA followed by Dunnett's multiple comparisons test (J, K, M, and N). All data error bars represent mean ± SEM. See also Figure S5.

- Subcellular fractionation and western blot
- Image processing, colocalization analysis and isosurface rendering
- FRET assays in HEK293 cells
- Behavioral profiling

- QUANTIFICATION AND STATISTICAL ANALYSIS
  - Data collection
  - Statistical analysis
- DATA AND SOFTWARE AVAILABILITY

SUPPLEMENTAL INFORMATION

Supplemental Information includes six figures, three tables, and one data file and can be found with this article online at https://doi.org/10.1016/j.celrep.2018.11.066.

ACKNOWLEDGMENTS

We thank Alon Chen, Rony Paz, and Avraham Yaron for helpful comments and discussions. We are indebted to Vladimir Kiss, Tali Shalit, and Nitzan Korem for

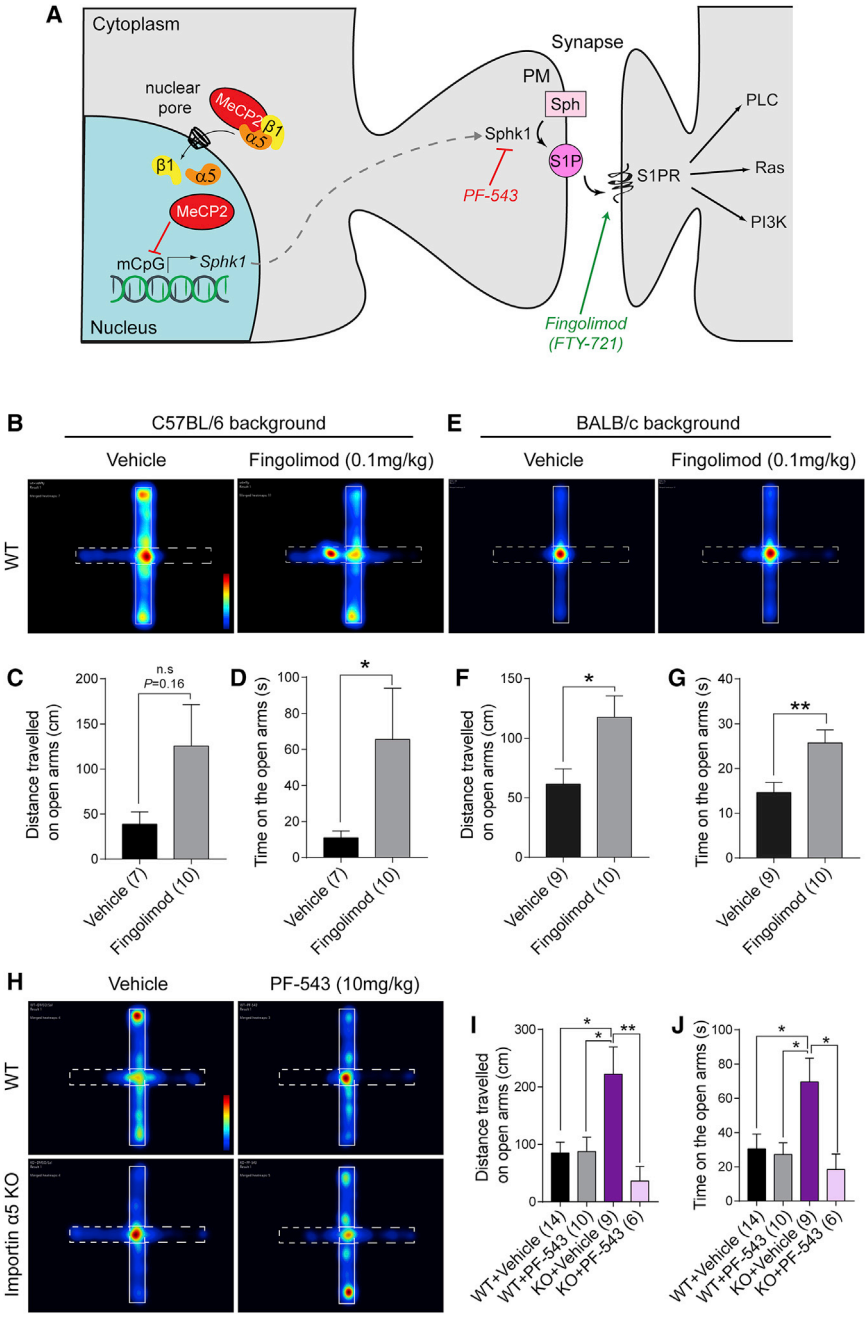

Figure 7. Importin α5 Regulates Anxiolysis through MeCP2 Nucleocytoplasmic Transport with Subsequent Effects on Lipid Signaling

(A) Schematic model of the proposed mechanism, indicating potential pharmacological challenges and their predicted outcomes.

(B–D) Density map of mouse exploratory activity in the elevated plus maze test showing the effects of fingolimod on wild-type C57BL/6 mice (B). Fingolimod has clear and robust anxiolytic effects, increasing the time spent in the open arms of the elevated plus maze (C and D).

(E–G) Density map of mouse exploratory activity in the elevated plus maze test showing the effects of fingolimod on wild-type BALB/c mice (E). Fingolimod treatment induced anxiolytic effects, increasing both the distance travelled (F) and the time spent (G) in the open arms of the elevated plus maze.

(H–J) Density map of mouse exploratory activity in the elevated plus maze (H) showing that the Sphk1 inhibitor PF-543 (10 mg/kg) reverses (I and J) the anxiety response of α5 knockouts toward wild-type values.

Average ± SEM, number of animals per group indicated in parentheses; *p < 0.05, **p < 0.01; two-tailed t test (C, D, F, and G) and one-way ANOVA followed by Tukey's HSD post hoc correction for multiple comparisons (I and J). All data error bars represent mean ± SEM. See also Figure S6.

excellent professional and technical assistance and to Yaniv Levi for devoted assistance with animal care. Our research was supported by the European Research Council (AdG Neurogrowth and PoC FAITh), a Simons Explorer Award (#437633), the Chaya Professorial Chair in Molecular Neuroscience (M.F.), the Carolito Stiftung Research Fellow Chair in Neurodegenerative Diseases (M.M.T.), and the French Ministry of Foreign Affairs International Volunteers Program and the Israel Ministry of Immigrant Absorption (N.P.).

AUTHOR CONTRIBUTIONS

N.P. performed the behavioral, molecular, and pharmacological experiments and stereotaxic surgeries and imaging. A.S. performed electrophysiological experiments. A.M. performed the FRET assays. N.P. and S.K. performed the subcellular fractionation and western blots. D.-A.S. produced the AAV vectors. N.P., A.S., S.Y.D., A.M., S.K., L.M., M.M.T., F.R., M.V., D.-A.S., B.E., E.R., E.H., M.B., I.M., and M.F. contributed to the concept and design of the experiments. N.P., A.S., S.Y.D., A.M., S.K., L.M., I.M., and M.F. collected, analyzed, or interpreted the data. N.P. and M.F. wrote the manuscript, with input from all coauthors.

DECLARATION OF INTERESTS

N.P. and M.F. have a pending patent application related to this work, PCT patent application number PCT/IL2018/050495 on "Methods of treating psychiatric stress disorders."

Received: May 25, 2017
Revised: October 9, 2018
Accepted: November 15, 2018
Published: December 11, 2018

REFERENCES

Baker, S.A., Lombardi, L.M., and Zoghbi, H.Y. (2015). Karyopherin α 3 and karyopherin α 4 proteins mediate the nuclear import of methyl-CpG binding protein 2. J. Biol. Chem. *290*, 22485–22493.

Bannerman, D.M., Sprengel, R., Sanderson, D.J., McHugh, S.B., Rawlins, J.N., Monyer, H., and Seeburg, P.H. (2014). Hippocampal synaptic plasticity, spatial memory and anxiety. Nat. Rev. Neurosci. *15*, 181–192.

Barnes, K.V., Coughlin, F.R., O'Leary, H.M., Bruck, N., Bazin, G.A., Beinecke, E.B., Walco, A.C., Cantwell, N.G., and Kaufmann, W.E. (2015). Anxiety-like behavior in Rett syndrome: characteristics and assessment by anxiety scales. J. Neurodev. Disord. *7*, 30.

Ben-Yaakov, K., Dagan, S.Y., Segal-Ruder, Y., Shalem, O., Vuppalanchi, D., Willis, D.E., Yudin, D., Rishal, I., Rother, F., Bader, M., et al. (2012). Axonal transcription factors signal retrogradely in lesioned peripheral nerve. EMBO J. *31*, 1350–1363.

Ch'ng, T.H., Uzgil, B., Lin, P., Avliyakulov, N.K., O'Dell, T.J., and Martin, K.C. (2012). Activity-dependent transport of the transcriptional coactivator CRTC1 from synapse to nucleus. Cell *150*, 207–221.

Chan, J.P., and Sieburth, D. (2012). Localized sphingolipid signaling at presynaptic terminals is regulated by calcium influx and promotes recruitment of priming factors. J. Neurosci. *32*, 17909–17920.

Chew, W.S., Wang, W., and Herr, D.R. (2016). To fingolimod and beyond: the rich pipeline of drug candidates that target S1P signaling. Pharmacol. Res. *113* (*Pt A*), 521–532.

Cooper, A., Grigoryan, G., Guy-David, L., Tsoory, M.M., Chen, A., and Reuveny, E. (2012). Trisomy of the G protein-coupled K+ channel gene, Kcnj6, affects reward mechanisms, cognitive functions, and synaptic plasticity in mice. Proc. Natl. Acad. Sci. USA *109*, 2642–2647.

Costes, S.V., Daelemans, D., Cho, E.H., Dobbin, Z., Pavlakis, G., and Lockett, S. (2004). Automatic and quantitative measurement of protein-protein colocalization in live cells. Biophys. J. *86*, 3993–4003.

Crawley, J.N. (2008). Behavioral phenotyping strategies for mutant mice. Neuron *57*, 809–818.

Dagan, S.Y., Tsoory, M.M., Fainzilber, M., and Panayotis, N. (2016). COLORcation: a new application to phenotype exploratory behavior models of anxiety in mice. J. Neurosci. Methods *270*, 9–16.

Deogracias, R., Yazdani, M., Dekkers, M.P., Guy, J., Ionescu, M.C., Vogt, K.E., and Barde, Y.A. (2012). Fingolimod, a sphingosine-1 phosphate receptor modulator, increases BDNF levels and improves symptoms of a mouse model of Rett syndrome. Proc. Natl. Acad. Sci. USA *109*, 14230–14235.

Dias, B.G., Banerjee, S.B., Goodman, J.V., and Ressler, K.J. (2013). Towards new approaches to disorders of fear and anxiety. Curr. Opin. Neurobiol. *23*, 346–352.

Dieterich, D.C., Karpova, A., Mikhaylova, M., Zdobnova, I., König, I., Landwehr, M., Kreutz, M., Smalla, K.H., Richter, K., Landgraf, P., et al. (2008). Caldendrin-Jacob: a protein liaison that couples NMDA receptor signalling to the nucleus. PLoS Biol. *6*, e34.

Evans, A.K., and Lowry, C.A. (2007). Pharmacology of the beta-carboline FG-7,142, a partial inverse agonist at the benzodiazepine allosteric site of the GABA A receptor: neurochemical, neurophysiological, and behavioral effects. CNS Drug Rev. *13*, 475–501.

Friedrich, B., Quensel, C., Sommer, T., Hartmann, E., and Köhler, M. (2006). Nuclear localization signal and protein context both mediate importin alpha specificity of nuclear import substrates. Mol. Cell. Biol. *26*, 8697–8709.

Gabel, H.W., Kinde, B., Stroud, H., Gilbert, C.S., Harmin, D.A., Kastan, N.R., Hemberg, M., Ebert, D.H., and Greenberg, M.E. (2015). Disruption of DNA-methylation-dependent long gene repression in Rett syndrome. Nature *522*, 89–93.

Gabriel, G., Klingel, K., Otte, A., Thiele, S., Hudjetz, B., Arman-Kalcek, G., Sauter, M., Shmidt, T., Rother, F., Baumgarte, S., et al. (2011). Differential use of importin-α isoforms governs cell tropism and host adaptation of influenza virus. Nat. Commun. *2*, 156.

Goffin, D., Allen, M., Zhang, L., Amorim, M., Wang, I.-T.J., Reyes, A.-R.S., Mercado-Berton, A., Ong, C., Cohen, S., Hu, L., et al. (2011). Rett syndrome mutation MeCP2 T158A disrupts DNA binding, protein stability and ERP responses. Nat. Neurosci. *15*, 274–283.

Gomez, C.M., Maselli, R., Gundeck, J.E., Chao, M., Day, J.W., Tamamizu, S., Lasalde, J.A., McNamee, M., and Wollmann, R.L. (1997). Slow-channel transgenic mice: a model of postsynaptic organellar degeneration at the neuromuscular junction. J. Neurosci. *17*, 4170–4179.

Griebel, G., and Holmes, A. (2013). 50 years of hurdles and hope in anxiolytic drug discovery. Nat. Rev. Drug Discov. *12*, 667–687.

Hanz, S., Perlson, E., Willis, D., Zheng, J.Q., Massarwa, R., Huerta, J.J., Koltzenburg, M., Kohler, M., van-Minnen, J., Twiss, J.L., and Fainzilber, M. (2003). Axoplasmic importins enable retrograde injury signaling in lesioned nerve. Neuron *40*, 1095–1104.

Herbst, W.A., and Martin, K.C. (2017). Regulated transport of signaling proteins from synapse to nucleus. Curr. Opin. Neurobiol. *45*, 78–84.

Imamura, T., Miyauchi-Senda, N., Tanaka, S., and Shiota, K. (2004). Identification of genetic and epigenetic similarities of SPHK1/Sphk1 in mammals. J. Vet. Med. Sci. *66*, 1387–1393.

Jeffrey, R.A., Ch'ng, T.H., O'Dell, T.J., and Martin, K.C. (2009). Activity-dependent anchoring of importin alpha at the synapse involves regulated binding to the cytoplasmic tail of the NR1-1a subunit of the NMDA receptor. J. Neurosci. *29*, 15613–15620.

Jimenez, J.C., Su, K., Goldberg, A.R., Luna, V.M., Biane, J.S., Ordek, G., Zhou, P., Ong, S.K., Wright, M.A., Zweifel, L., et al. (2018). Anxiety cells in a hippocampal-hypothalamic circuit. Neuron *97*, 670–683.

Kaddoum, L., Panayotis, N., Mazarguil, H., Giglia-Mari, G., Roux, J.C., and Joly, E. (2013). Isoform-specific anti-MeCP2 antibodies confirm that expression of the e1 isoform strongly predominates in the brain. F1000Res. *2*, 204.

Kanno, T., Nishizaki, T., Proia, R.L., Kajimoto, T., Jahangeer, S., Okada, T., and Nakamura, S. (2010). Regulation of synaptic strength by sphingosine 1-phosphate in the hippocampus. Neuroscience *171*, 973–980.

Karpova, A., Mikhaylova, M., Bera, S., Bär, J., Reddy, P.P., Behnisch, T., Rankovic, V., Spilker, C., Bethge, P., Sahin, J., et al. (2013). Encoding and transducing the synaptic or extrasynaptic origin of NMDA receptor signals to the nucleus. Cell *152*, 1119–1133.

Kempf, A., Tews, B., Arzt, M.E., Weinmann, O., Obermair, F.J., Pernet, V., Zagrebelsky, M., Delekate, A., Iobbi, C., Zemmar, A., et al. (2014). The sphingolipid receptor S1PR2 is a receptor for Nogo—a repressing synaptic plasticity. PLoS Biol. *12*, e1001763.

Koch, M. (1999). The neurobiology of startle. Prog. Neurobiol. *59*, 107–128.

Lim, A.F., Lim, W.L., and Ch'ng, T.H. (2017). Activity-dependent synapse to nucleus signaling. Neurobiol. Learn. Mem. *138*, 78–84.

Livak, K.J., and Schmittgen, T.D. (2001). Analysis of relative gene expression data using real-time quantitative PCR and the 2(-Delta Delta C(T)) method. Methods *25*, 402–408.

Lyst, M.J., and Bird, A. (2015). Rett syndrome: a complex disorder with simple roots. Nat. Rev. Genet. *16*, 261–275.

Lyst, M.J., Ekiert, R., Guy, J., Selfridge, J., Koerner, M.V., Merusi, C., De Sousa, D., and Bird, A. (2018). Affinity for DNA contributes to NLS independent nuclear localization of MeCP2. Cell Rep. *24*, 2213–2220.

Matsuura, K., Kabuto, H., Makino, H., and Ogawa, N. (1997). Pole test is a useful method for evaluating the mouse movement disorder caused by striatal dopamine depletion. J. Neurosci. Methods *73*, 45–48.

Miyamoto, Y., Yamada, K., and Yoneda, Y. (2016). Importin α: a key molecule in nuclear transport and non-transport functions. J. Biochem. *160*, 69–75.

Moreau, T., Bungener, C., Heinzlef, O., Suchet, L., Borgel, F., Bourdeix, I., Meite, M., Rerat, K., and Chouette, I.; GRACE Study Group (2017). Anxiety and coping strategy changes in multiple sclerosis patients initiating fingolimod: The GRACE prospective study. Eur. Neurol. *77*, 47–55.

Mühle, C., Reichel, M., Gulbins, E., and Kornhuber, J. (2013). Sphingolipids in psychiatric disorders and pain syndromes. Handb. Exp. Pharmacol. *216*, 431–456.

Müller, C.P., Reichel, M., Mühle, C., Rhein, C., Gulbins, E., and Kornhuber, J. (2015). Brain membrane lipids in major depression and anxiety disorders. Biochim. Biophys. Acta *1851*, 1052–1065.

Murrough, J.W., Yaqubi, S., Sayed, S., and Charney, D.S. (2015). Emerging drugs for the treatment of anxiety. Expert Opin. Emerg. Drugs *20*, 393–406.

Na, E.S., Nelson, E.D., Adachi, M., Autry, A.E., Mahgoub, M.A., Kavalali, E.T., and Monteggia, L.M. (2012). A mouse model for MeCP2 duplication syndrome: MeCP2 overexpression impairs learning and memory and synaptic transmission. J. Neurosci. *32*, 3109–3117.

Neufeld-Cohen, A., Tsoory, M.M., Evans, A.K., Getselter, D., Gil, S., Lowry, C.A., Vale, W.W., and Chen, A. (2010). A triple urocortin knockout mouse model reveals an essential role for urocortins in stress recovery. Proc. Natl. Acad. Sci. USA *107*, 19020–19025.

Oliverio, A., Eleftheriou, B.E., and Bailey, D.W. (1973). A gene influencing active avoidance performance in mice. Physiol. Behav. *11*, 497–501.

Panayotis, N., Karpova, A., Kreutz, M.R., and Fainzilber, M. (2015). Macromolecular transport in synapse to nucleus communication. Trends Neurosci. *38*, 108–116.

Perry, R.B., Doron-Mandel, E., Iavnilovitch, E., Rishal, I., Dagan, S.Y., Tsoory, M., Coppola, G., McDonald, M.K., Gomes, C., Geschwind, D.H., et al. (2012). Subcellular knockout of importin β1 perturbs axonal retrograde signaling. Neuron *75*, 294–305.

Prut, L., and Belzung, C. (2003). The open field as a paradigm to measure the effects of drugs on anxiety-like behaviors: a review. Eur. J. Pharmacol. *463*, 3–33.

Pumroy, R.A., and Cingolani, G. (2015). Diversification of importin-α isoforms in cellular trafficking and disease states. Biochem. J. *466*, 13–28.

Rafael, J.A., Nitta, Y., Peters, J., and Davies, K.E. (2000). Testing of SHIRPA, a mouse phenotypic assessment protocol, on Dmd(mdx) and Dmd(mdx3cv) dystrophin-deficient mice. Mamm. Genome *11*, 725–728.

Ramocki, M.B., Peters, S.U., Tavyev, Y.J., Zhang, F., Carvalho, C.M.B., Schaaf, C.P., Richman, R., Fang, P., Glaze, D.G., Lupski, J.R., and Zoghbi, H.Y. (2009). Autism and other neuropsychiatric symptoms are prevalent in individuals with MeCP2 duplication syndrome. Ann. Neurol. *66*, 771–782.

Rishal, I., and Fainzilber, M. (2014). Axon-soma communication in neuronal injury. Nat. Rev. Neurosci. *15*, 32–42.

Rother, F., Shmidt, T., Popova, E., Krivokharchenko, A., Hügel, S., Vilianovich, L., Ridders, M., Tenner, K., Alenina, N., Köhler, M., et al. (2011). Importin α7 is essential for zygotic genome activation and early mouse development. PLoS ONE *6*, e18310.

Saito, A., and Cavalli, V. (2016). Signaling over distances. Mol. Cell. Proteomics *15*, 382–393.

Samaco, R.C., Fryer, J.D., Ren, J., Fyffe, S., Chao, H.T., Sun, Y., Greer, J.J., Zoghbi, H.Y., and Neul, J.L. (2008). A partial loss of function allele of methyl-CpG-binding protein 2 predicts a human neurodevelopmental syndrome. Hum. Mol. Genet. *17*, 1718–1727.

Samaco, R.C., Mandel-Brehm, C., McGraw, C.M., Shaw, C.A., McGill, B.E., and Zoghbi, H.Y. (2012). Crh and Oprm1 mediate anxiety-related behavior and social approach in a mouse model of MECP2 duplication syndrome. Nat. Genet. *44*, 206–211.

Schnute, M.E., McReynolds, M.D., Kasten, T., Yates, M., Jerome, G., Rains, J.W., Hall, T., Chrencik, J., Kraus, M., Cronin, C.N., et al. (2012). Modulation of cellular S1P levels with a novel, potent and specific inhibitor of sphingosine kinase-1. Biochem. J. *444*, 79–88.

Shmidt, T., Hampich, F., Ridders, M., Schultrich, S., Hans, V.H., Tenner, K., Vilianovich, L., Qadri, F., Alenina, N., Hartmann, E., et al. (2007). Normal brain development in importin-alpha5 deficient-mice. Nat. Cell Biol. *9*, 1337–1338, author reply 1339.

Stearns, N.A., Schaevitz, L.R., Bowling, H., Nag, N., Berger, U.V., and Berger-Sweeney, J. (2007). Behavioral and anatomical abnormalities in Mecp2 mutant mice: a model for Rett syndrome. Neuroscience *146*, 907–921.

Suzuki, K., Bose, P., Leong-Quong, R.Y., Fujita, D.J., and Riabowol, K. (2010). REAP: A two minute cell fractionation method. BMC Res. Notes *3*, 294.

Terenzio, M., Koley, S., Samra, N., Rishal, I., Zhao, Q., Sahoo, P.K., Urisman, A., Marvaldi, L., Oses-Prieto, J.A., Forester, C., et al. (2018). Locally translated mTOR controls axonal local translation in nerve injury. Science *359*, 1416–1421.

Thompson, K.R., Otis, K.O., Chen, D.Y., Zhao, Y., O'Dell, T.J., and Martin, K.C. (2004). Synapse to nucleus signaling during long-term synaptic plasticity; a role for the classical active nuclear import pathway. Neuron *44*, 997–1009.

Tovote, P., Fadok, J.P., and Lüthi, A. (2015). Neuronal circuits for fear and anxiety. Nat. Rev. Neurosci. *16*, 317–331.

Trullas, R., and Skolnick, P. (1993). Differences in fear motivated behaviors among inbred mouse strains. Psychopharmacology (Berl.) *111*, 323–331.

Ushijima, R., Sakaguchi, N., Kano, A., Maruyama, A., Miyamoto, Y., Sekimoto, T., Yoneda, Y., Ogino, K., and Tachibana, T. (2005). Extracellular signal-dependent nuclear import of STAT3 is mediated by various importin alphas. Biochem. Biophys. Res. Commun. *330*, 880–886.

Walf, A.A., and Frye, C.A. (2007). The use of the elevated plus maze as an assay of anxiety-related behavior in rodents. Nat. Protoc. *2*, 322–328.

West, A.E., and Greenberg, M.E. (2011). Neuronal activity-regulated gene transcription in synapse development and cognitive function. Cold Spring Harb. Perspect. Biol. *3*, a005744.

Yasuhara, N., Shibazaki, N., Tanaka, S., Nagai, M., Kamikawa, Y., Oe, S., Asally, M., Kamachi, Y., Kondoh, H., and Yoneda, Y. (2007). Triggering neural differentiation of ES cells by subtype switching of importin-alpha. Nat. Cell Biol. *9*, 72–79.

Yasuhara, N., Yamagishi, R., Arai, Y., Mehmood, R., Kimoto, C., Fujita, T., Touma, K., Kaneko, A., Kamikawa, Y., Moriyama, T., et al. (2013). Importin alpha subtypes determine differential transcription factor localization in embryonic stem cells maintenance. Dev. Cell *26*, 123–135.

Yudin, D., Hanz, S., Yoo, S., Iavnilovitch, E., Willis, D., Gradus, T., Vuppalanchi, D., Segal-Ruder, Y., Ben-Yaakov, K., Hieda, M., et al. (2008). Localized regulation of axonal RanGTPase controls retrograde injury signaling in peripheral nerve. Neuron *59*, 241–252.

STAR★METHODS

KEY RESOURCES TABLE

REAGENT or RESOURCE	SOURCE	IDENTIFIER
Antibodies		
MECP2-e1 (rabbit)	E. Joly lab (Kaddoum et al., 2013)	N/A
MECP2-e1+e2 (rabbit)	E. Joly lab (Kaddoum et al., 2013)	N/A
HDAC3 (rabbit)	Abcam	RRID:AB_443297
GFP (rabbit)	MBL International	RRID:AB_10597267
RFP (rabbit)	Rockland	RRID:AB_2209751
T7 (goat)	Abcam	RRID:AB_307038
Alexa Fluor 488 secondary antibody (Donkey anti-rabbit)	Thermo Fisher Scientific	RRID:AB_2556546
Alexa Fluor 546 secondary antibody (Donkey anti-rabbit)	Thermo Fisher Scientific	RRID:AB_2534016
Alexa Fluor 546 secondary antibody (Donkey anti-goat)	Thermo Fisher Scientific	RRID:AB_2534103
DAPI (4.6-diamino-2-phenolindol dihydrochloride)	Thermo Fisher Scientific	RRID:AB_2629482
Bacterial and Virus Strains		
pAAV-CaMKII-ArchT-GFP backbone	Edward Boyden lab (MIT)	Addgene plasmid #37807
pAAV-shRNA-ctrl backbone	Hongjun Song lab (Johns Hopkins U School of Medicine)	Addgene plasmid #85741
AAV5-CaMKII-T7-(human Kpna1 ORF)	This paper	N/A
AAV5-U6-sh (mouse Kpna1)-Venus	This paper	N/A
AAV5-U6-sh (Scramble)-Venus	This paper	N/A
FUGW 3rd gen lentiviral plasmid with hUbC-driven EGFP	David Baltimore lab (Caltech)	Addgene Plasmid #14883
Lenti-U6-shKpna1-hSyn-3NLS-eRFP	Charité U Viral Core	https://vcf.charite.de/en/
Lenti-U6-shScramble-hSyn-3NLS-eRFP	Charité U Viral Core	https://vcf.charite.de/en/
Chemicals, Peptides, and Recombinant Proteins		
FG-7142	Sigma-Aldrich	Cat#E006-100MG
PF-543	Cayman Chemicals	Cat#17034
Fingolimod (FTY-720)	Sigma-Aldrich	Cat#SML0700-5MG
Critical Commercial Assays		
RNA extraction kit: RNAqueous-Micro Kit	Ambion / Life Technologies	Cat#AM1931
AAVpro Purification Kit (all serotypes)	Takara Bio	Cat#6666
Deposited Data		
Expression profiling by high throughput sequencing	GEO (Gene Expression Omnibus) database	GSE106546
Experimental Models: Cell Lines		
HEK293	ATCC	RRID:CVCL_0045
Experimental Models: Organisms/Strains		
Mouse / C57BL/6OlaHsd	Harlan Israel	N/A
Mouse / BALB/c	Harlan Israel	N/A
Mouse / C57BL/6OlaHsd / Importin $\alpha1^{-/-}$	Gabriel et al., 2011; Rother et al., 2011; Shmidt et al., 2007	N/A
Mouse / C57BL/6OlaHsd / Importin $\alpha3^{-/-}$	Gabriel et al., 2011; Rother et al., 2011; Shmidt et al., 2007	N/A
Mouse / C57BL/6OlaHsd / Importin $\alpha4^{-/-}$	Gabriel et al., 2011; Rother et al., 2011; Shmidt et al., 2007	N/A
Mouse / C57BL/6OlaHsd / Importin $\alpha5^{-/-}$	Gabriel et al., 2011; Rother et al., 2011; Shmidt et al., 2007	N/A
Mouse / C57BL/6OlaHsd / Importin $\alpha7^{-/-}$	Gabriel et al., 2011; Rother et al., 2011; Shmidt et al., 2007	N/A

(*Continued on next page*)

Continued

REAGENT or RESOURCE	SOURCE	IDENTIFIER
Oligonucleotides		
See Table S3	IDT (Integrated DNA Technologies)	N/A
Recombinant DNA		
shRNA_Kpna1 used in lenti (GCAACACAGAAGTTTAGGAAA)	Metabion International AG, Germany	N/A
sh-Scramble used in lenti (TTCGCACCCTACTTCGTGG)	Metabion International AG, Germany	N/A
shRNA_Kpna1 used in AAV5 (GCAACACAGAAGTTTAGGAAATT)	IDT (Integrated DNA Technologies)	N/A
sh-Scramble used in AAV5 (TTCGCACCCTACTTCGTGGTT)	IDT (Integrated DNA Technologies)	N/A
pDEST-hMeCP2-GFP	Huda Y. Zoghbi lab (Baylor College of Medicine)	Addgene plasmid #48078
pCMVTNT-T7-KPNA1	Bryce Paschal lab (University of Virginia)	Addgene plasmid #26677
pmScarlet-i_C1	Dorus Gadella lab (University of Amsterdam)	Addgene plasmid #85044
Software and Algorithms		
Ethovision XT 10	Noldus	RRID:SCR_000441
VideoMot2	TSE Systems	RRID:SCR_014334
COLORcation	Fainzilber lab (Dagan et *al*., 2016)	N/A
TRANSFAC (TF binding site analysis)	geneXplain	RRID:SCR_005573
Prism v7 for Windows	GraphPad Software, La Jolla, California, USA	RRID:SCR_002798
Fiji	NIH	RRID:SCR_002285
IMARIS (v7.7.2)	Bitplane AG	RRID:SCR_007370
Other		
Fluoromount-G® (mounting solution)	SouthernBiotech	Cat#0100-01

CONTACT FOR REAGENT AND RESOURCES SHARING

Further information and requests for resources and reagents should be directed to and will be fulfilled by the Lead Contact, Mike Fainzilber (mike.fainzilber@weizmann.ac.il).

EXPERIMENTAL MODEL AND SUBJECT DETAILS

Animal Subjects

All animal procedures were approved by the IACUC of the Weizmann Institute of Science. Importin α single mutants for importin α1, α3, α4, α5 and α7 were generated by conventional gene deletion strategies (Gabriel et al., 2011; Rother et al., 2011; Shmidt et al., 2007). C57BL/6 or BALB/c mice were from Harlan (Israel). Mice were kept at 24.0 ± 0.5°C in a humidity-controlled room under a 12-h light–dark cycle with free access to food and water. Experiments were carried out on 2-5 months old male mice, unless specified otherwise.

METHOD DETAILS

Pharmacological treatments

All drugs were administered by intraperitoneal injection (I.P.). FG-7142 (Sigma-Aldrich, #E006-100MG) was used as an anxiolytic drug, and administered as described previously (Evans and Lowry, 2007) at a final concentration of 5 mg/kg body weight 30 min before behavioral testing. The SphK1 antagonist PF-543 (Cayman Chemicals, #17034) was dissolved in 2% DMSO/PBS 0.01M and administered at a final dosage of 10mg/kg. Fingolimod (FTY-720, Sigma-Aldrich, #SML0700-5MG) was used as an S1P receptor agonist, dissolved in saline solution and administered at a final dosage of 0.1 mg/kg, as described (Deogracias et al., 2012).

Hippocampal slice preparation

Hippocampal slice recordings were used to investigate the impact of importin α5 deletion at the circuit level. To do so, 8-10 week-old mice were deeply anesthetized with isoflurane, followed by decapitation. The brains were removed and the horizontal hippocampal slices (300-350 μm) were prepared with a Vibratome (Ci 7000 smz, Campden instruments Ltd.) in the ice-cold cutting ACSF solution

(215 mM sucrose, 20 mM glucose, 26 mM $NaHCO_3$, 2.5 mM KCl, 1.6 mM NaH_2PO_4, 1 mM $CaCl_2$, 4 mM $MgSO_4$, 4 mM $MgCl_2$). After sectioning, the slices were transferred to the ACSF solution (124 mM NaCl, 10 mM glucose, 26 mM NaHCO3, 2.5 mM KCl, 1 mM NaH2PO4, 2.5 mM CaCl2, 0.65 mM MgSO4) and incubated for 1 - 1.5 hours at room temperature under constant oxygenation.

Electrophysiology

Slices were transferred into an interface recording chamber with constant perfusion of warm (32°C) oxygenated ACSF. Input-output relationship (I/O curve) was assessed by stimulation of the Schaffer collaterals with a custom-made constant current stimulus isolator; the stimulus intensity varied from 0 to 500 μA, the length of stimulation was 0.1 ms. The field excitatory postsynaptic potentials (fEPSP) were recorded by positioning 3-5 MΩ glass pipette in *stratum radiatum* of the CA1 hippocampal region. The fEPSPs were amplified, filtered by AC-coupled amplifier (Grass Instrument Co., West Warwick, RI) with a bandwidth of 0.1 Hz - 3 kHz and acquired at 10 kHz with a NI-6341 A/D converter (National Instruments, Austin, TX) and WinWCP software (Dr. J. Dempster, University of Strathclyde).

For the analysis, the I/O curves of the basal synaptic transmission were fitted using Boltzman charge-voltage equation to calculate the stimulation that produces the half-maximal fEPSP response (half-maximal stimulation intensity): $f(I) = (max-min)/(1+exp((I_{1/2}-I)/s))+min$, where *max* & *min* – maximal and minimal responses, respectively, $I_{1/2}$ – stimulation that produces 50% of maximal response, *I* – stimulation intensity, *s* – slope of rise. For paired-pulse and LTP experiments, the stimulation current was adjusted to about half-maximal stimulation intensity. For the paired-pulse protocol, at least 5 consecutive recordings were acquired for each stimulation interval The LTP was induced by two trains of high-frequency stimulations (HFS, 100 Hz for 1 s) with a 20 s inter-train interval. The LTP usually lasted for 1.5 hr. Changes of fEPSP were evaluated by measurement of slope between 10% and 90% of the peak response (linear fit). All data were analyzed in IGOR Pro.6.04 (Wavemetrics, Oregon, USA) using custom-written macros for normalization, fitting and averaging of data and statistical tests. To quantify the changes in synaptic strength in response to HFS paradigm, the slopes of the post-stimulation fEPSPs were normalized to the fEPSP slopes of baseline recordings (set at 100%). One way ANOVA followed by Holm-Sidak post hoc analysis was used for statistical comparisons of mean fEPSP slopes, with a minimal significance level of $p < 0.05$. 5-6 slices from different animals were used for each recording.

Lentiviral and AAVs vector design and production

Viral vectors were used for knockdown or re-expression of importin α5, as needed. The Lenti-shα5 vector sequences were selected by cross-referencing the BiOSETTIA shRNA designer (http://biosettia.com/support/shrna-designer) and the MISSION® shRNA library from Sigma. Briefly, two different short hairpin RNA (shRNA) target sequences from the open reading frame of the mouse importin α5 gene (Kpna1) were cloned into shRNA expression cassettes using BamHI/PacI restriction sites driven by the u6 promoter in a modified third-generation lentiviral plasmid with hUBC-driven EGFP (FUGW was from the Baltimore lab at Caltech, Addgene plasmid #14883) with 3x-NLS RFP fluorescent reporter driven under human synapsin (hSyn) promoter. RT-qPCR and western blot analyses were used to select the most appropriate shRNAs, based on their ability to specifically knockdown importin α5.

AAV5 vectors were used to carry out both knockdown and re-expression experiments with similar viruses. To this end, we cloned a shRNA target sequence of the mouse importin α5 gene (Kpna1) as well as a scramble control sequence into an AAV ITR vector driven by the u6 promoter with a fluorescent eYFP (Venus) reporter. The re-expression construct was generated by cloning the human importin α5 (Kpna1) sequence under the CaMKII promoter with an addition of a 5′prime T7 tag into an AAV ITR vector. Recombinant AAV5 vectors expressing shRNA and hKpna1 were produced by transfecting HEK293T cells using the AAVpro helper-free systems. AAV5 viral preparations were purified using the AAVpro® Purification Kit (All Serotypes; Takara Bio. Inc., Cat#6666).

Intracerebral injections of lentiviral vectors and AAVs

In order to evaluate the impact of acute knockdown and re-expression of importin α5 on anxiety-related behaviors we performed a series of stereotaxic injections in adult mice. Nine weeks-old C57BL/6J male mice (Envigo, Israel) received bilateral stereotaxic injections of lentivirus carrying a shRNA targeting the murine form of importin α5/Kpna1 (Lenti-U6-shKpna1-hSyn-3NLS-eRFP, n = 13) or its scramble control sequence (n = 9) into the ventral hippocampus (1 μL lentivirus per side, 0.1 μl. min^{-1}). Similarly, nine weeks-old C57BL/6J male mice (Envigo, Israel) received bilateral stereotaxic injections of AAV5-u6-shKpna1-Venus (n = 8 mice) or the AAV5-u6-scramble-Venus (n = 8 mice) into the ventral hippocampus (1 μl per side, 0.1 μl min^{-1}). Finally, eight adult mice were used for the rescue experiment and received a combination of two viruses: 1) one expressing the shα5 targeting the murine importin α5 (AAV5-u6-shKpna1-Venus) and one expressing the human importin α5/Kpna1 ORF (AAV5-CaMKII-T7-hKpna1ORF). 10 other mice received a combination of AAV5-u6-scramble-Venus with the AAV5-CaMKII-T7-hKpna1ORF expression construct, solely as a readout of importin α5 gene expression. Mice were anesthetized with isoflurane and placed on a computer-guided stereotaxic apparatus (Angle Two Stereotaxic Instrument, myNeurolab, Leica Microsystems Inc., Bannockburn, IL, USA), which is integrated with the Paxinos and Franklin mouse brain atlas through a control panel. The viral vectors were delivered using a 2 μl Hamilton syringe connected to a motorized nano-injector. To allow diffusion of the solution into the brain tissue, the needle was left in place for 5 min before and after the injection (coordinates, relative to bregma: AP = −3.2 mm, L = ± 3.2 mm, H = −3.8 mm, based on a calibration experiment indicating these coordinates as leading to the ventral hippocampus in C57BL/6 strain). The mice recovered from the surgery for a period of 3 weeks before behavioral testing. Following behavioral tests, confirmation of the knockdown or rescue of importin α5 was done by RT-qPCR. Animals showing no knockdown were discarded from the analysis. Validation of the injection for the lenti-shKpna1 was

done by immunostaining using a rabbit anti-RFP antibody, for the AAV5-shKpna1 versus AAV5-scramble by immunostaining using a rabbit anti-GFP antibody and for the AAV5 carrying the hKpna1ORF by immunostaining using a goat anti-T7 antibody (see Immunofluorescence method section). The stained slides were screened for fluorescence at the injection sites and representative images taken. The mice that did not show fluorescent labeling at the aimed injection location were excluded from the data.

RNA expression analysis (RNA-Seq)

We carried out RNA-seq analyses to assess the impact of importin α5 deletion on the hippocampal transcriptome. Total RNA was extracted from hippocampi dissected from either importin α5 or wild-type animals treated with vehicle or the anxiogenic compound FG-7142. Intraperitoneal injections of vehicle or drug were done 30 minutes prior to dissection (4 experimental groups, 3 animals per each group and replicate, 3 replicates of the entire set) using the RNAqueous-Micro Kit (Ambion) according to manufacturer's instructions. Replicates of high RNA integrity (RIN $\geq$ 7) were processed for RNA-Seq on an Illumina HiSeq (read type: SR60_V4) at the Crown Institute for Genomics (G-INCPM, Weizmann Institute of Science). Data was analyzed using DESeq software and have been deposited in NCBI's Gene Expression Omnibus (GEO) and are accessible through GEO series accession number: GSE106546.

Library Construction and Sequencing

500 ng of total RNA for each sample, from three independent experiments, was processed using the TruSeq RNA sample preparation Kit v2 protocol (Illumina). Libraries were evaluated by Qubit and TapeStation. Sequencing Libraries were constructed with barcodes to allow multiplexing of 12 samples on 4 lanes of Illumina HiSeq machine, using the Single-Read 50 protocol (v3). The output was ~88.5 million reads per sample. FastQ files for each sample were generated by the usage of Illumina CASAVA-1.8.2 software.

Sequence Data/ Bioinformatics Analysis

Reads for each sample, were aligned independently using TopHat2 (v2.0.10) against the mouse genome (GRCm38). The percentage of the reads that were aligned uniquely to the genome was ~92%. Counting proceeded over genes annotated in RefSeq release mm10, using HTseq-count (version 0.6.1p1). Only uniquely mapped reads were used to determine the number of reads falling into each gene (intersection-strict mode). Differential analysis was performed using DESeq package (1.18.0) with the betaPrior, cooksCutoff and independentFiltering parameters set to False. Differentially expressed genes, were determined by a p value of < 0.05 and absolute fold changes > 1.5 and max raw counts > 10. Differential expressed (DE) genes were analyzed through the use of Ingenuity Pathways Analysis (Ingenuity® Systems, https://www.qiagenbioinformatics.com/) to determine most significantly relevant biological functions and pathways.

Gene expression analysis by RT-qPCR

Total RNA from mouse brain tissue was extracted using the Ambion RNAqueous-Micro total RNA isolation kit (Life Technologies Corp.). RNA purity, integrity (RIN > 7) and concentration was determined, and 100 ng of total RNA was then used to synthesize cDNA using SuperScript III (Invitrogen). RT-qPCR was performed on a ViiA7 System (Applied Biosystems) using PerfeCTa SYBR Green (Quanta Biosciences, Gaithersburg, USA). Forward/Reverse primers were designed for different exons, and the RNA was treated with DNase H to avoid false-positives. Amplicon specificity was verified by melting curve analysis. All RT-qPCR reactions were conducted in technical triplicates and the results were averaged for each sample, normalized to *Actb* levels and the relevant reporter genes such as *RFP*, *GFP* and *T7* for the viruses, and analyzed using the comparative ΔΔCt method (Livak and Schmittgen, 2001). The primers (*Mus musculus*) that were used are listed in Table S3.

Transcription Factor Binding Site (TFBS) analysis

We assessed possible enrichment of different TFBS in datasets of regulated genes using FMatch (geneXplain) on gene sets with fold changes of 1.5 or more and their corresponding background sets. Promoter sequences from the importin α5 dataset and a list of background genes (non-deregulated genes) were scanned from 600 base pairs (bp) upstream to 100 bp downstream of the predicted transcription start site for each such gene, and TFBS were identified with TRANSFAC 9. TFBS enrichment in test versus background sets was assessed by t test with *p-value* threshold of 0.05.

Immunofluorescence

We used immunofluorescence in order to assess the subcellular localization of MeCP2 within neurons in different brain areas. Briefly, mice were deeply anaesthetized with pentobarbital (100 mg/kg) and transcardially perfused (NaCl for 1 min, followed by 4% paraformaldehyde/PBS 1x for 10 min). Brains were removed and postfixed for 5 h and cryoprotected in 20% sucrose for another 24 h, then frozen at −80°C before cryostat sectioning (20 μm coronal sections). Slices containing sections of cortex (motor cortex), hippocampus (both ventral and dorsal) and amygdala were collected in separate sets for immunohistochemistry, so that each set contained every fifth serial section. Briefly, sections were rehydrated, permeabilized (0.1% Triton X-100 PBS 1X), blocked (7% normal donkey serum) and incubated overnight at room temperature with the appropriate primary antibody: Rabbit anti-MECP2-e1 (1:1000 (Kaddoum et al., 2013)), Rabbit anti-GFP (1:4000, MBL International Cat# 598-7), Rabbit-anti-RFP (1:1000, Rockland Cat# 600-401-379), Goat anti-T7 (1:1000, Abcam ab9138). Sections were subsequently incubated with the secondary antibody: donkey anti-rabbit (Alexa 488 or Alexa 546) or donkey anti-goat Alexa 546 (1:200, Thermo Fisher Scientific), DAPI (4',6-diamino-2-phenolindol

dihydrochloride) counterstaining was performed on all sections, in order to visualize the nucleus and then mounted with Fluoromount-G® (SouthernBiotech, Cat#0100-01).

Subcellular fractionation and western blot

We performed subcellular fractionation prior to western blot analysis to test if lack of importin α5 reduces MeCP2 nuclear localization. Analyses were performed on ventral hippocampus and amygdala as these brain regions have been implicated in anxiety-related behaviors. Microdissected tissues were flash frozen in liquid nitrogen before preparation of subcellular fractions using the REAP protocol (Suzuki et al., 2010). The tissue was dissociated in 400 μL fractionation solution (0.1% NP40, Calbiochem, CA, USA) in PBS using a glass tissue douncer and 100 μL of it kept as "input." The remaining 300 μL was centrifuged for 5 min at 500 G in 1.5 mL microcentrifuge tubes and 200 μL of the supernatant kept as the "cytosolic fraction." The pellet was resuspended in 400 μL fractionation solution and re-centrifuged for 5 min at 500 G before discarding the supernatant, and resuspending the "nuclear fraction" pellet in 400 μL (ventral hippocampus) or 40 μL (amygdala) TRIS buffer. These nuclear fractions were further processed for western blotting. Protein concentrations were estimated using the BCA method according to the manufacturer's protocol. Equal amounts of protein samples were boiled in 5x Laemmli sample buffer, fractionated by SDS-PAGE and transferred to nitrocellulose membrane using a Bio-Rad transfer apparatus according to the manufacturer's protocol. Membranes were incubated for 1 h at room temperature in blocking solution 5% nonfat milk in TBST (10 mM Tris, pH 8.0, 150 mM NaCl, 0.5% Tween 20). After incubation, the membranes were washed 3 times (15 minutes each) and incubated with the Rabbit anti-MeCP2 antibody (Kaddoum et al., 2013; 1:4000) and Rabbit anti-HDAC3 (1:1000; Abcam AB160471) for overnight at 4°C. Membranes were washed 4 times for 15 minutes and incubated with a 1:10000 dilution of HRP-conjugated anti-mouse or anti-rabbit antibodies for 1 h. Membranes were washed 4 times for 10 minutes in TBST and images were captured with the ECL system (Amersham Biosciences) according to the manufacturer's protocols and the signal quantified using the *Fiji* software (http://fiji.sc).

Image processing, colocalization analysis and isosurface rendering

Images were acquired on an Olympus FV1000 inverted confocal (Olympus, Tokyo) with Fluoview (FV10–ASW 4.1) software. In general, brain slices were scanned using camera settings identical for all genotypes in a given experiment. Images were imported into the *Fiji* version (http://fiji.sc) of the *ImageJ* software for threshold subtraction and subsequent analyses (see below).

Colocalization analysis

The nuclear localization of MeCP2 was determined by colocalization analyses. Fiji contains a panel of preinstalled plugins including a procedure for colocalization analysis, designated as "Colocalization Threshold," which calculates a variety of colocalization parameters such as the Mander's colocalization coefficient (Costes et al., 2004) based on pixel intensity correlation measurements. The background of both channels (MeCP2 and DAPI) was subtracted. The channels were equalized to the intensity range to compensate for potential intensity differences between the channels. Then, the "Colocalization Threshold" plugin was run without a region of interest or mask. Numerical correlation parameters were recorded, as well as the 2D intensity histogram for visualization of the correlation between the two channels.

Isosurface rendering

For higher resolution analyses of MeCP2 localization we used high-resolution 60x confocal image stacks of areas of interest (ventral hippocampus, dorsal hippocampus, Amygdala, Cortex M1/M2) labeled for MeCP2 and DAPI and reconstructed them by using the isosurface rendering plugin of the IMARIS software (version 7.7.2, Bitplane AG).

FRET assays in HEK293 cells

FRET acceptor photobleaching experiments were performed to study the interaction of MeCP2 with importin α5. Briefly, HEK293 cells were grown in 35 mm cell culture plates and transfected with 1) MeCP2-GFP + importin α5-mScarlet-I in separate plasmids or in the control conditions 2) cytoplasmic-GFP + importin α5-mScarlet-I or 3) PTE (phosphotriesterase)-GFP + importin α5-mScarlet-I; 12 h prior to the experiment cells were split on 24 mm cover glass coated with poly-L-lysine. Imaging was done in PBS solution containing calcium and magnesium (Sigma). Experiments were performed on the Olympus FV1000 inverted confocal microscope described above. GFP was excited with 488 nm laser line and mScarlet-I with 561 nm laser line. The acceptor (mScarlet-I) was bleached with 561 nm laser at maximal power setting. The FRET efficiency (E_{FRET}, %) was analyzed using the *Fiji* software and calculated as $E_{FRET} = (D_{post} + D_{pre})/D_{post}$ x 100 with D being the donor (GFP) fluorescence before (pre) and after (post) acceptor bleaching.

Behavioral profiling

All assays were performed during the "dark" active phase of the diurnal cycle under dim illumination (~10lx) unless otherwise stated; the ventilation system in the test rooms provided a ~65 dB white noise background. Every daily session of testing started with a 2 hr habituation period to the test rooms. A recovery period of at least 1 day was provided between the different behavioral assays.

Home-cage locomotion test

Home-cage locomotor activity was monitored over 72 consecutive hours using the InfraMot system (TSE Systems, Germany) in order to investigate possible alterations of basal activity and/or circadian rythms. The system tracks the spatial displacement of body-heat images (infra-red radiation) over time (Cooper et al., 2012; Neufeld-Cohen et al., 2010). The first 24 h were used as a habituation phase. The last 48h (2 consecutive dark/light cycles) were analyzed and the corresponding mouse activity calculated.

Open field

Motility and anxiety-like behaviors were assayed in the open-field (Cooper et al., 2012; Neufeld-Cohen et al., 2010). The total distance moved (cm), the time spent (global, center, border; s), center/border ratio, mean speed (cm/s), percentage of time spent moving versus rest in the different defined area were recorded using VideoMot2 (TSE System, Germany) or Ethovision XT11 (Noldus Information Technology, the Netherlands). Open-field was performed under 120lx for the assessment of anxiety-related behaviors or 6lx for the study of general locomotion. Open-field raw data were further analyzed with *COLOR*cation (Dagan et al., 2016), allowing the unbiased study of mice activity based on group heat-maps.

Elevated plus maze

The elevated plus maze was used as a proxy for anxiety and risk-taking behaviors. The elevated plus maze consists of two open arms and two enclosed ones connected by a central square. Exploration on the open arms is reduced in high anxiety states while it is increased in low anxiety states (Walf and Frye, 2007). Mice were placed on the central platform facing one of the ''open'' arms to initiate a 5-min test session and the time spent in each arm was measured. The test was performed under 7 lx and 65 dB white noise. The number of entries into, the time spent/distance on the open arms and the percentage of the open arm entries compared with total number of arm entries are were recorded using the VideoMot2 software (TSE System, Germany) or the Ethovision XT11 software (Noldus Information Technology, the Netherlands).

Acoustic startle reflex (ASR)

Rodent ASR is a major body muscle contraction response to a loud and abrupt sound. Enhanced ASR is a hallmark of increased fear and/or sustained anxiety (Koch, 1999). An ASR apparatus (StartleResponse, TSE Systems, Germany) consisting of a sound-attenuated, well-ventilated cabinet was used. Sessions started with a 5-min acclimation period with background white noise (65 dB) maintained throughout. During the last 2 minutes of this period an individual activity baseline was recorded. Overall, 32 startle stimuli (120 dB, 40 ms; inter-trials interval: randomly varying, 12–30 s) were presented; the stimuli presentation was divided into three 'Blocks': Blocks 1 and 3 consisted of 6 startle stimuli each, whereas Block 2 consisted of 10 startle stimuli and 10 'no stimuli' (65 dB (A), 40 ms; i.e., equivalent to the background white noise) that were presented in a quasi-random manner. Two indices were recorded for each of the blocks: (1) RT ASR (ms) = mean reaction time to respond to the startle stimuli (latency to exceed the individual activity baseline). (2) The average response amplitude produced in response to the startling stimuli, and (3) the latency to reach the maximal response (ms).

Morris water maze

We studied possible alterations of spatial memory in the Morris water maze. The water maze consisted of a circular tank (120 cm diameter) with a removable escape platform centered in one of the four maze quadrants. In the testing room, only distal visual-spatial cues for locating the hidden platform were available. During testing, the tank is filled with 24°C water clouded with milk powder. *Acquisition phase*. The mice were subjected to 4 trials per day with an inter-trial interval of 10 mins, for 5 consecutive days. In each trial, the mice were required to find a platform located in one of the four quadrant submerged 1 cm below the water surface. The escape latency in each trial was recorded up to 90 s. Each mouse was allowed to remain on the platform for 15 s and was then removed from the maze. If the mouse did not escape in the allocated time, it was manually placed on the platform for 15 s. *Probe test*. Memory was assessed 24 hours after the last trial. The escape platform was removed and mice were allowed to search for it for 1 minute; and the time spent, the swimming distance in the different quadrants of the pool and the time spent (percentage) and the number of crossing over the virtual platform location was monitored using an automated tracking system (VideoMot2, TSE Systems, Germany).

Fear conditioning

The fear conditioning paradigm was used to study possible alteration of hippocampal or amygdala-dependent forms of memories. A computer-controlled fear-conditioning system (TSE Systems, Germany) monitors the procedure while measuring freezing behavior (i.e., lack of movement except respiration). The test is performed within three days as previously described (Neufeld-Cohen et al., 2010): 1) *Habituation*: on the first day, mice are habituated for 5 min to the fear conditioning chamber, a clear Plexiglas cage (21 cm × 20 cm × 36 cm) with a stainless steel floor grid within a constantly illuminated (250 lx) fear-conditioning housing. 2) *Conditioning*: conditioning takes place on day 2 in one 5-min training session. Mice initially explore the context for 2 min. Thereafter, two pairings of a co-terminating tone [conditioned stimulus (CS): 30 s, 3,000 Hz, pulsed 10 Hz, 80 dB (A)] and shock [unconditioned stimulus (US): 0.7 mA, 2 s, constant current) with a fixed ITI of 60 s. The US is delivered through the metal grid floor. Mice are removed from this chamber 1 min after the last CS–US pairing. The chamber is cleaned with 10% ethanol before each session. The ventilating fan of the conditioning box housing provides a constant auditory background noise [white noise, 62 dB(A)]. 3) *Testing*: Context dependent memory is tested 24 h after the conditioning by re-exposure to the conditioning box for 5 min without any stimuli. The Cue dependent memory is tested 1 h after the Context test by exposure to the conditioned [conditioned stimulus (CS): 30 s, 3,000 Hz, pulsed 10 Hz, 80 dB (A)] in different environmental conditions (black Plexiglas box, black floor instead of metal grid, no illumination, no ventilation noise, cleaning solution: acetic acid 10% instead of alcohol 10%).

Accelerated rotarod

We assessed the integrity of balance and coordination with the ROTOR-ROD system (83x91x61 - SD. Instruments, San Diego). This test is used to measure motor coordination and balance in mice (Crawley, 2008). Mice were subjected to 3 trials, with 5 min inter-trial intervals. Rotarod acceleration was set at 20rpm in 240 s. Latency to fall (sec) was recorded and the average of the 3 trials was used as an index of motor coordination and balance.

Wire hanging

The wire hanging test examines motor neuromuscular impairment and motor coordination (Gomez et al., 1997; Rafael et al., 2000). Forepaws of the tested mouse were allowed to grasp and hold the animal suspended on an elevated metal wire (diameter = 2mm, length = 90cm) 80 cm above a water-filled tank. Traction was determined as the ability not to drop from the wire and to remain stable and hanging. The time (sec) until the mouse completely releases its grip was recorded.

Pole test

The pole test assesses basal ganglia-related movement disorders in mice (Matsuura et al., 1997). Briefly, mice are placed head-up on top of a 50 cm-long horizontal pole (1 cm in diameter). The base of the pole was placed in the home cage. When the pole was flipped downward, animals orient themselves (turn) and descend the length of the pole back into their home cage. Mice received 2d of training that consisted of five trials for each session. On the test day, animals received five trials, and time to orient downward T_{Turn} was recorded. If mouse was not able to turn or fell, a cutoff value of 120 s was attributed.

QUANTIFICATION AND STATISTICAL ANALYSIS

Data collection

No statistical methods were used to pre-determine sample sizes which were similar to those reported in previous works. Data collection and analysis were performed blind to the conditions of the experiment. All mice were assigned randomly to the different experimental groups.

Statistical analysis

A normality test (Shapiro-Wilk test) was applied to all data before analysis for statistical significance. Datasets which passed the normality test were subjected to parametric analysis. Analysis of multiple groups was made using the ANOVA method. The choice between one- or two-way ANOVA was based on the requirements for identification of specific factors' contribution to statistical differences between groups and were followed by the Tukey and the Sidak post hoc analysis tests respectively. For 2-groups analyses, unpaired Student's t test was used. Datasets that did not pass the normality test were subjected to nonparametric analysis using the Kruskal-Wallis test on rank for multiple-group statistical evaluation followed by Dunn's multiple comparisons test. For 2-groups analyses, the Mann-Whitney test was used. Potential outliers were discarded using the ROUT method with a Q (maximum desired false discovery rate) of 1%. All analyses were performed using GraphPad Prism version 7.00 for Windows (GraphPad Software, La Jolla, California, USA, https://www.graphpad.com/). The results are expressed as the mean ± standard error of the mean (SEM). All statistical parameters for specific analyses are reported in the figure legends of the paper. Statistically significant *P*-values are shown as $^{*}p < 0.05$, $^{**}p < 0.01$, $^{***}p < 0.001$ and $^{****}p < 0.0001$.

DATA AND SOFTWARE AVAILABILITY

Gene expression analysis (RNA-seq) data generated from this paper have been deposited in NCBI's Gene Expression Omnibus (GEO) and are accessible through GEO series accession number: GSE106546.

Cell Reports, Volume *25*

Supplemental Information

Importin α5 Regulates Anxiety through MeCP2 and Sphingosine Kinase 1

Nicolas Panayotis, Anton Sheinin, Shachar Y. Dagan, Michael M. Tsoory, Franziska Rother, Mayur Vadhvani, Anna Meshcheriakova, Sandip Koley, Letizia Marvaldi, Didi-Andreas Song, Eitan Reuveny, Britta J. Eickholt, Enno Hartmann, Michael Bader, Izhak Michaelevski, and Mike Fainzilber

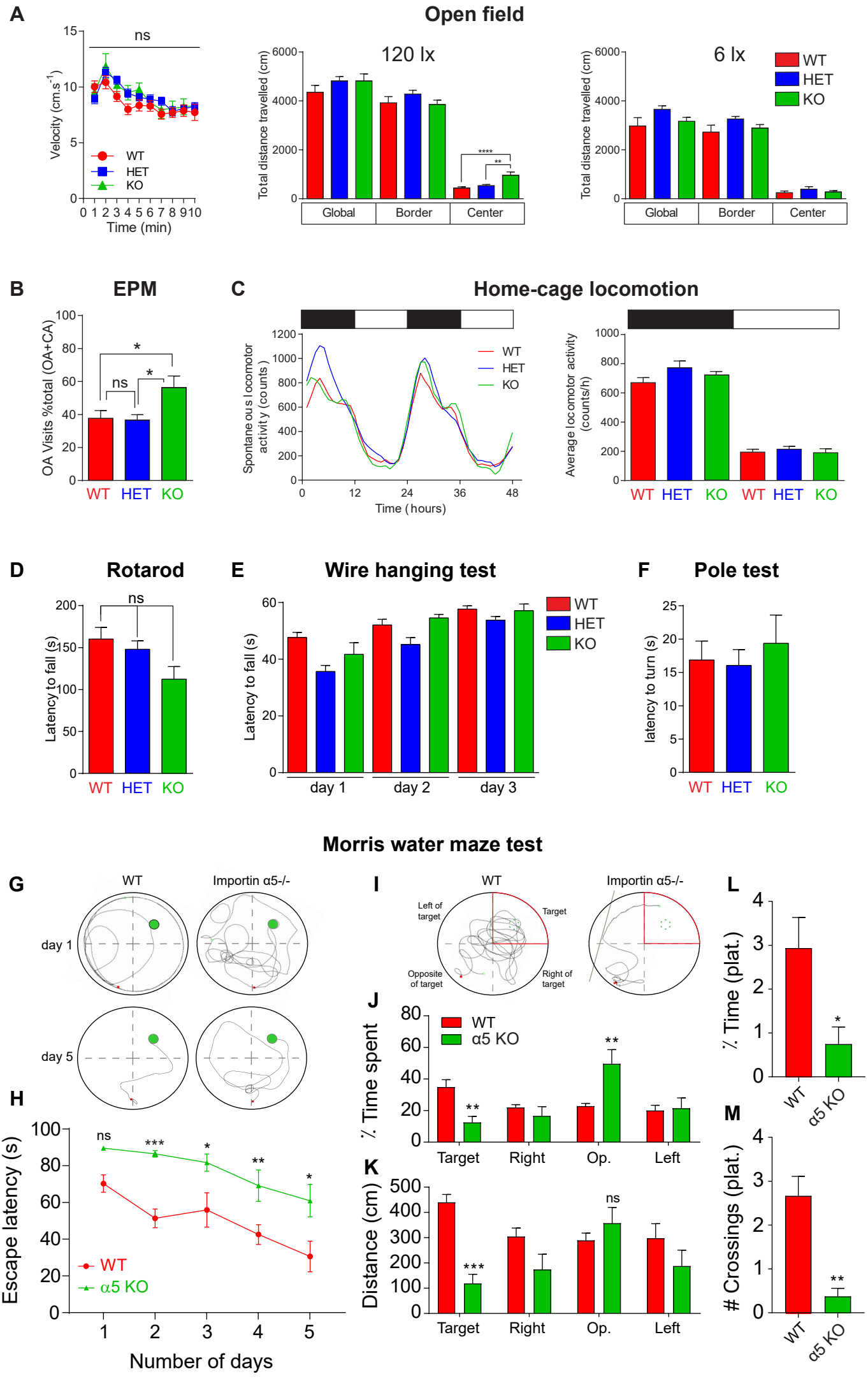
A
Open field
ns
Velocity (cm.s-1)
Time (min)
WT
HET
KO
120 lx
6 lx
Total distance travelled (cm)
Global
Border
Center
B
EPM
OA Visits %total (OA+CA)
C
Home-cage locomotion
Spontaneous locomotor activity (counts)
Time (hours)
Average locomotor activity (counts/h)
D
Rotarod
Latency to fall (s)
E
Wire hanging test
day 1
day 2
day 3
F
Pole test
latency to turn (s)
Morris water maze test
G
WT
Importin α5-/-
day 1
day 5
H
Escape latency (s)
Number of days
α5 KO
I
Left of target
Target
Opposite of target
Right of target
J
% Time spent
Target
Right
Op.
Left
K
Distance (cm)
L
% Time (plat.)
M
Crossings (plat.)

Fig. S1 (*Related to Fig. 2*)**. Preserved sensory and motor performance and impaired Morris water maze performances in importin α5 knockout mice. A**, importin α5 KO movement speed (green) was not significantly different over the 10 min of the OF session compared to WT (red) and HET (blue) littermates. Reducing OF illumination from 120 to 6 lux abolished differences between WT and importin α5 KO animals in the distance travelled in the OF center area. **B**, importin α5 KO mice show increased exploration of EPM open arms (expressed as a percentage of open arm visits from the total number of visits to all arms) ($p < 0.05$). **C**, Circadian activity over 48 hrs shows that the home-cage activity of importin α5 KO was not different from WT and HET during the dark and light phases (black and white boxes above the graphs, respectively). **D**, accelerated rotarod, **E**, wire hanging test and **F**, pole test, all confirm the absence of locomotion and coordination/balance defects in importin α5 KO animals. $n \geq 6$ animals for each genotype per test. **G-H**, Importin α5 knockout mice showed altered performance during the spatial acquisition phase of the Morris water maze. Mice were subjected to 4 trials per day with an interval of 10 min, for 5 consecutive days (See Methods). G, Representative swimming paths for each genotype at day 1 and day 5 (end of acquisition). The green circle depicts the location of the hidden platform and the dashed lines demarcates the 4 quadrants. H, Escape latency (in seconds) over time during training sessions in the Morris water maze. **I-M**, Importin α5 knockout do not actively search for the escape platform. **I**, Representative swimming paths for the probe test session (24hrs after acquisition – dashed green circles mark where the hidden platform was located during training and the target quadrant appears in red). **J**, The percentage time spent in each of the quadrants during the probe test (target, right of target, opposite of target, left of target) shows that importin α5 knockout spent less time scanning the target quadrant while they spent more time in the opposite one compared to their wild-type littermates. **K**, The distance covered during the probe test suggests that importin α5 knockouts explore the target quadrant less, but do not compensate by swimming more in the other quadrants during the session. **L**, Percentage time spent and **M**, Number of crossing over the platform location. n=9 WT; n=8 Importin α5 KO. * $p < 0.05$; ** $p < 0.01$, *** $p < 0.001$ (one-way ANOVA followed by Tukey's HSD post hoc correction for multiple comparisons (**A-F**); Two-way ANOVA followed by Sidak post-hoc analysis test (**H, J, K**) and Mann-Whitney test (**L, M**)). All data error bars represent mean +/- SEM.

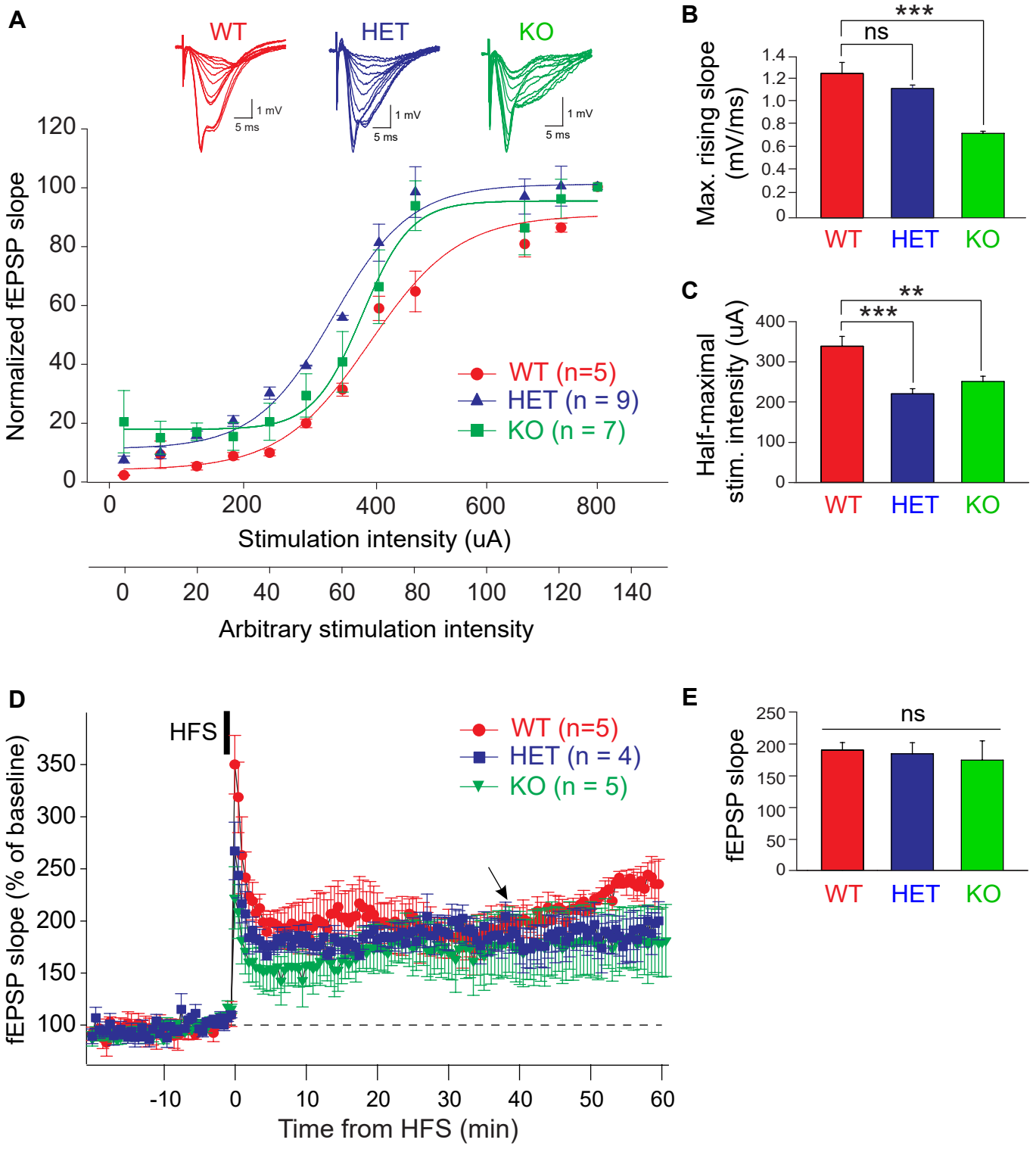
A
WT
HET
KO
1 mV
5 ms
Normalized fEPSP slope
Stimulation intensity (uA)
Arbitrary stimulation intensity
WT (n=5)
HET (n = 9)
KO (n = 7)
B
Max. rising slope (mV/ms)
ns
***
C
Half-maximal stim. intensity (uA)
**
***
D
HFS
fEPSP slope (% of baseline)
Time from HFS (min)
WT (n=5)
HET (n = 4)
KO (n = 5)
E
fEPSP slope
ns

Fig. S2 (*Related to Fig. 3*)**. Electrophysiological analyses in importin α5 knockout hippocampus. A-C**, Input-output relationship between the stimulation magnitude and synaptic response enhancement during basal synaptic activity. **A**, top: representative raw data traces obtained from WT, HET and importin α5 KO mice respectively. Bottom: relationship between the intensity of the presynaptic current and the slope of fEPSP response normalized to the absolute maximal fEPSP slope in each group shown in (**B**) as the maximum change in potential: $[(\mathrm{dV/dt})\mathrm{Max} \equiv \mathrm{dVmax/dt}]$. The absolute maximal fEPSP slope is significantly reduced in importin α5 KOs. **C**, The half-maximal stimulation intensity is reduced both in HET and KO. The half-maximal stimulation intensity was derived from sigmoidal fit equation $\left(\mathrm{W} = \mathrm{Wmax}/\left(1 - \mathrm{e}^{(-\mathrm{I}1/2)}/\mathrm{a}\right)\right) + \mathrm{const.}$, where $\mathrm{W} = \mathrm{dV/dt}$, $\mathrm{Wmax} = \mathrm{dVmax/dt}$, $\mathrm{I}\,1/2$ is the half-maximal stimulation intensity and a is the sigmoidal function slope. **D, E**, LTP experiment. **D**, Summary of 1 hr LTP recordings from hippocampal slices of WT, HET, and KO mice. The LTP was estimated as a stable increase in fEPSP slope after high frequency stimulation (HFS) composed of two 1 s-long trains of 100 Hz given at time point 0 (HFS and black bold arrow). **E**, Representative normalized fEPSP magnitudes sampled at 42 min after HFS application (black diagonal arrow pointing to the time point). n=5 (WT), 9 (HET), and 7 (α5 KO). ** $p < 0.01$, *** $p < 0.001$ (One way ANOVA with Holm-Sidak post-hoc analysis).

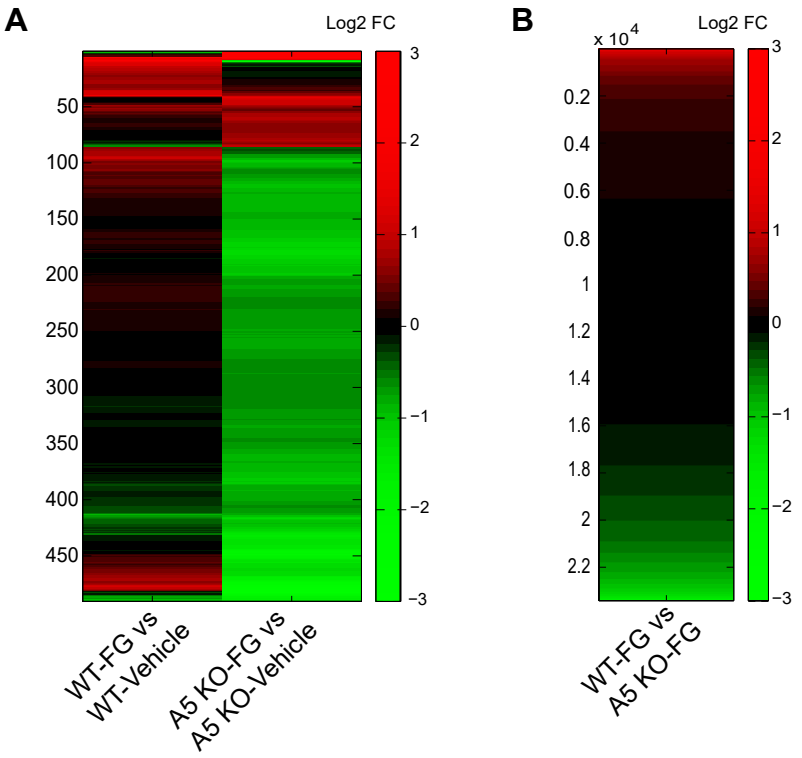

C **Top Networks (Ingenuity)**

1. Organismal Development, Connective Tissue Development and Function, Skeletal and Muscular System
2. Development and Function / Connective Tissue Disorders, Developmental Disorder, Hereditary Disorder
3. Cancer, Organismal Injury and Abnormalities, Reproductive System Disease
4. Molecular Transport, Lipid Metabolism, Small Molecule Biochemistry
5. Inflammatory Disease, Ophthalmic Disease, Organismal Injury and Abnormalities

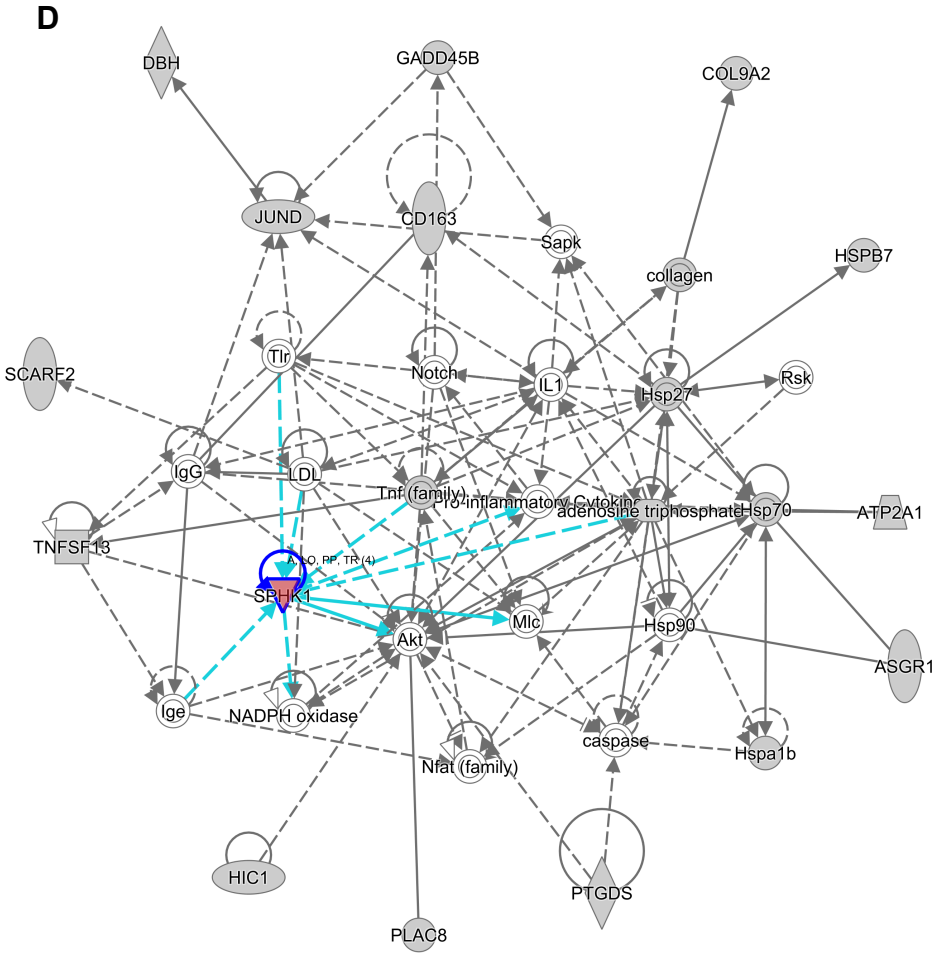

Fig. S3 (*Related to Fig. 5*)**. RNA-seq and network analyses. A**, Heat maps showing log2-normalized fold-change of gene expression in WT+FG vs WT vehicle, α5+FG vs α5-vehicle and **B**, the comparison of WT-FG with α5-FG revealing a larger cohort of almost 600 transcripts that were differentially regulated by FG7142 treatment in knockout versus wild type mice (n = 3 mice per group). See also Table S2. **C**, Identification of signaling networks using the Ingenuity Pathway Analysis program and the candidate genes from the top ranked pathway. **D**, the lipid metabolism network identified as one of the top five signaling networks by Ingenuity contains the Sphk1 gene (red triangle) upregulated in α5 hippocampi.

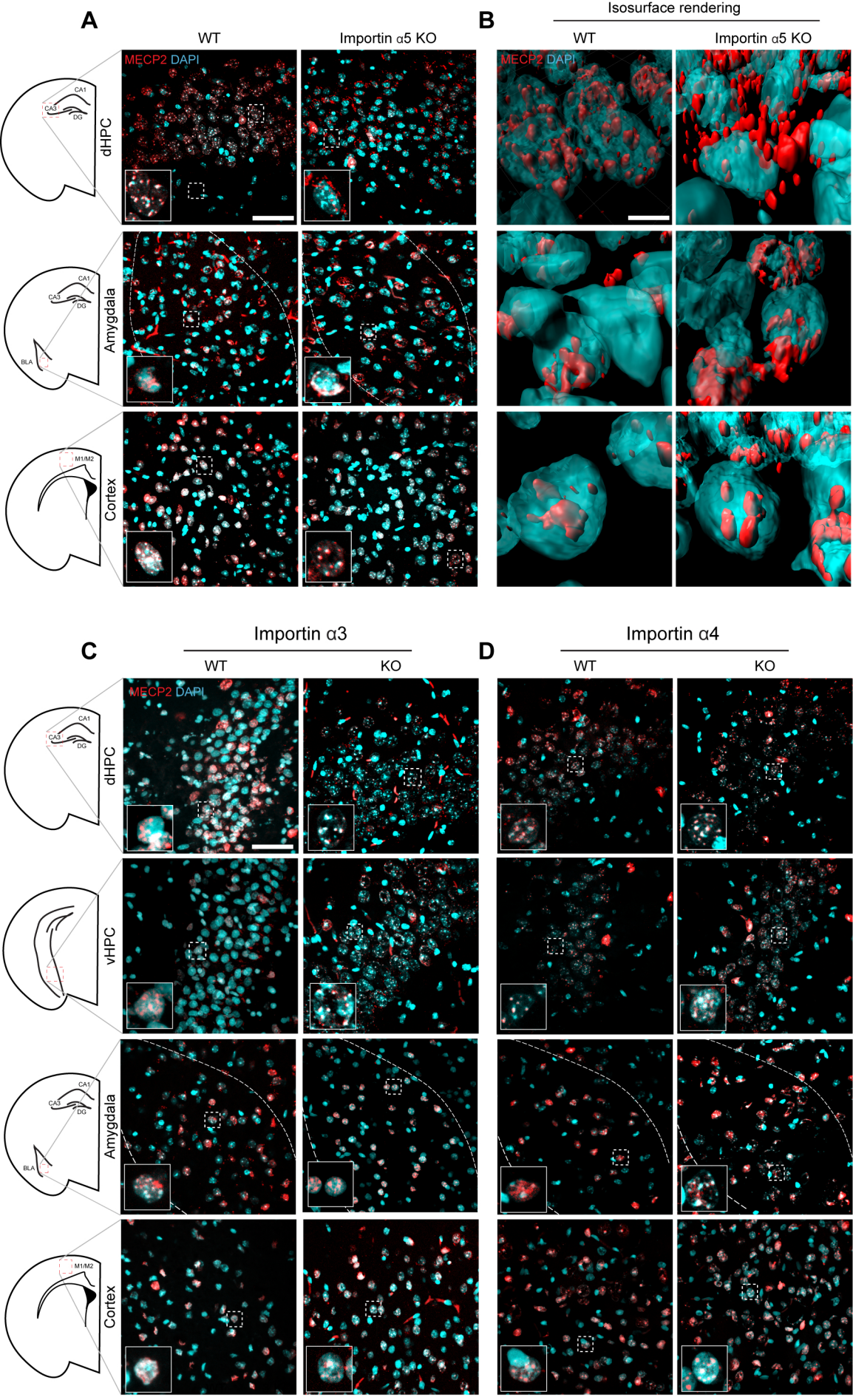
A
WT
Importin α5 KO
MECP2 DAPI
dHPC
Amygdala
Cortex
CA1
CA3
DG
BLA
M1/M2
B
Isosurface rendering
WT
Importin α5 KO
MECP2 DAPI
C
Importin α3
WT
KO
MECP2 DAPI
dHPC
vHPC
Amygdala
Cortex
D
Importin α4
WT
KO
E
WT
α3 KO
Mecp2-DAPI coloc.
(Mander's coefficient m1)
1.0
0.8
0.6
0.4
0.2
0.0
ns
Cortex
dHPC
vHPC
Amyg.
F
WT
α4 KO
Mecp2-DAPI coloc.
(Mander's coefficient m1)
ns
Cortex
dHPC
vHPC
Amyg.

Fig. S4 (*Related to Fig. 5*)**. MeCP2-DAPI colocalization analyses in importin α-deleted brain regions. A,** Immunofluoresence for MECP2 (red) and DAPI nuclear staining (blue) revealing a punctate heterochromatic pattern in neuronal nuclei in the dorsal hippocampus (dHPC; CA3 region), the amygdala and the motor cortex of WT mice, with reduced colocalization in importin α5 knockout dorsal hippocampus while no significant differences were observed in the amygdala and the cortex. **B**, Isosurface rendering of the neuronal nuclei in the respective brain regions (scale bar 50 μm in A and 10 μm in B). **C, D,** Immunofluoresence for MECP2 and DAPI in WT and importin α3 (**C**) and importin α4 (**D**) knockout brain areas and the respective colocalization analyses showing no difference in the subcellular localization of MeCP2 in importin in α3 (**E**) and α4 (**F**) brains (Mander's coefficient m1, $n \geq 3$ for per genotype and per structure). All data error bars represent mean +/- SEM.

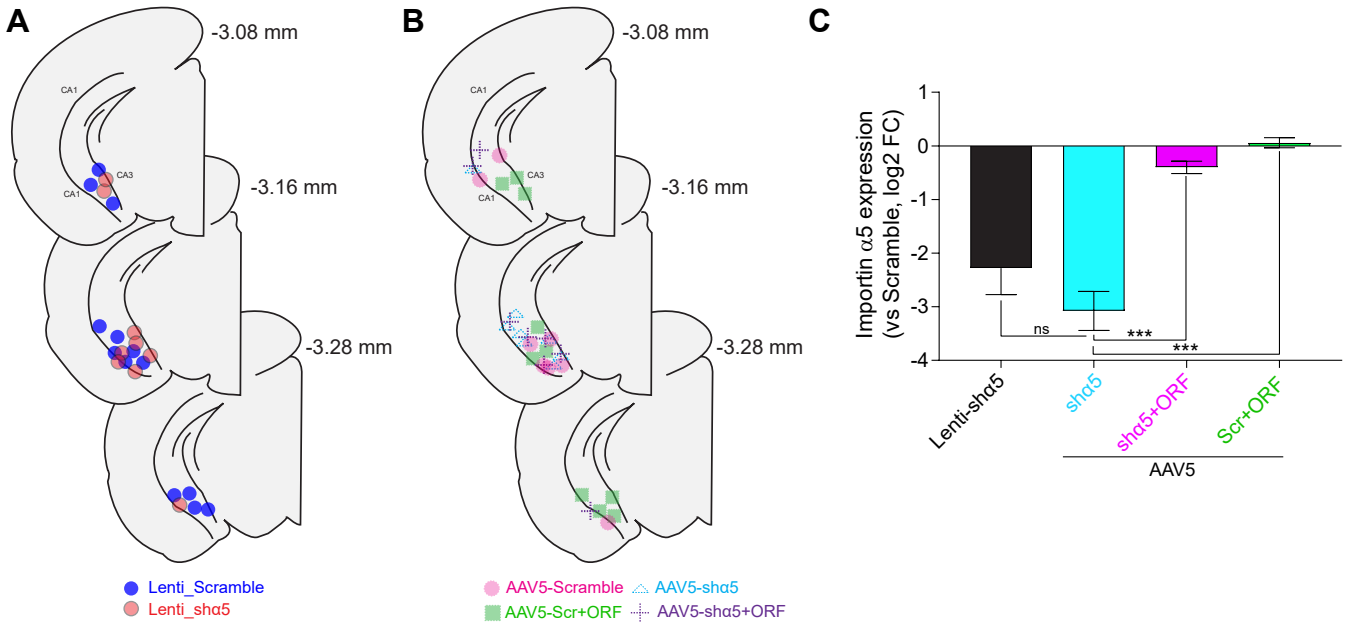
A
-3.08 mm
-3.16 mm
-3.28 mm
CA1
CA3
Lenti_Scramble
Lenti_shα5
B
-3.08 mm
-3.16 mm
-3.28 mm
AAV5-Scramble
AAV5-shα5
AAV5-Scr+ORF
AAV5-shα5+ORF
C
Importin α5 expression (vs Scramble, log2 FC)
ns
***
***
Lenti-shα5
shα5
shα5+ORF
Scr+ORF
AAV5

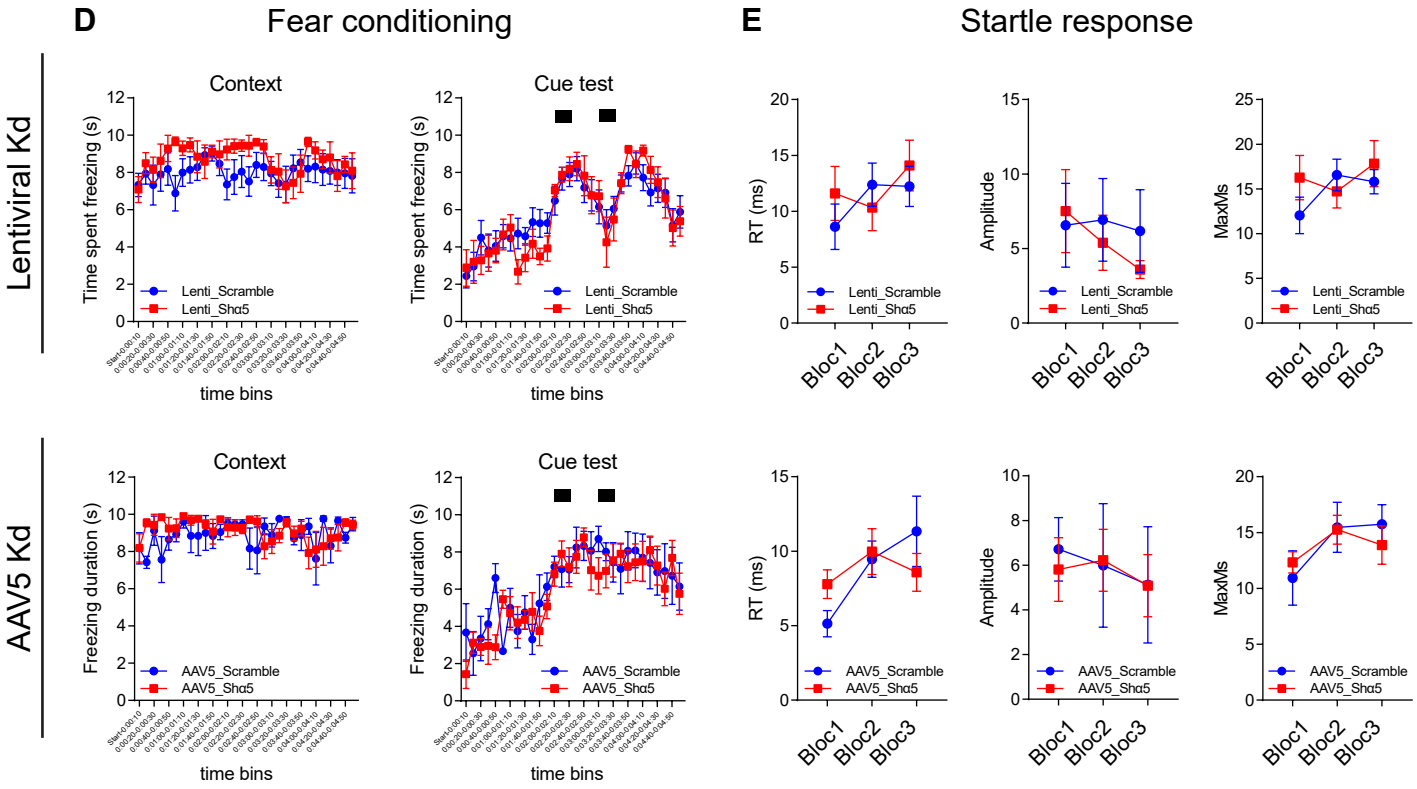
D
Fear conditioning
E
Startle response
Lentiviral Kd
AAV5 Kd
Context
Cue test
Time spent freezing (s)
Freezing duration (s)
time bins
Lenti_Scramble
Lenti_Shα5
AAV5_Scramble
AAV5_Shα5
RT (ms)
Amplitude
MaxMs
Bloc1
Bloc2
Bloc3

Fig. S5 (*Related to Fig. 6*)**. Acute knockdown of importin α5. A, B,** Schematic representation of the virus injection position in the ventral hippocampus. The brain plates illustrating the injection sites were designed in accordance to the Paxinos and Franklin Mouse Brain Atlas (distance from Bregma are shown in mm). **C,** RT-qPCR results showing the knockdown of importin α5 in the vHPC 5 weeks after injection (after completion of behavioral study) of the respective virus preparations. Results expressed as log2 fold-change vs. the respective scramble-injected control condition. *** $p < 0.001$ (Unpaired two-tailed *t*-test). Panels **D, E** respectively show the absence of differences in the fear conditioning freezing behavior and startle response of Lentivirus and AAV5-injected mice. All data error bars represent mean +/- SEM.

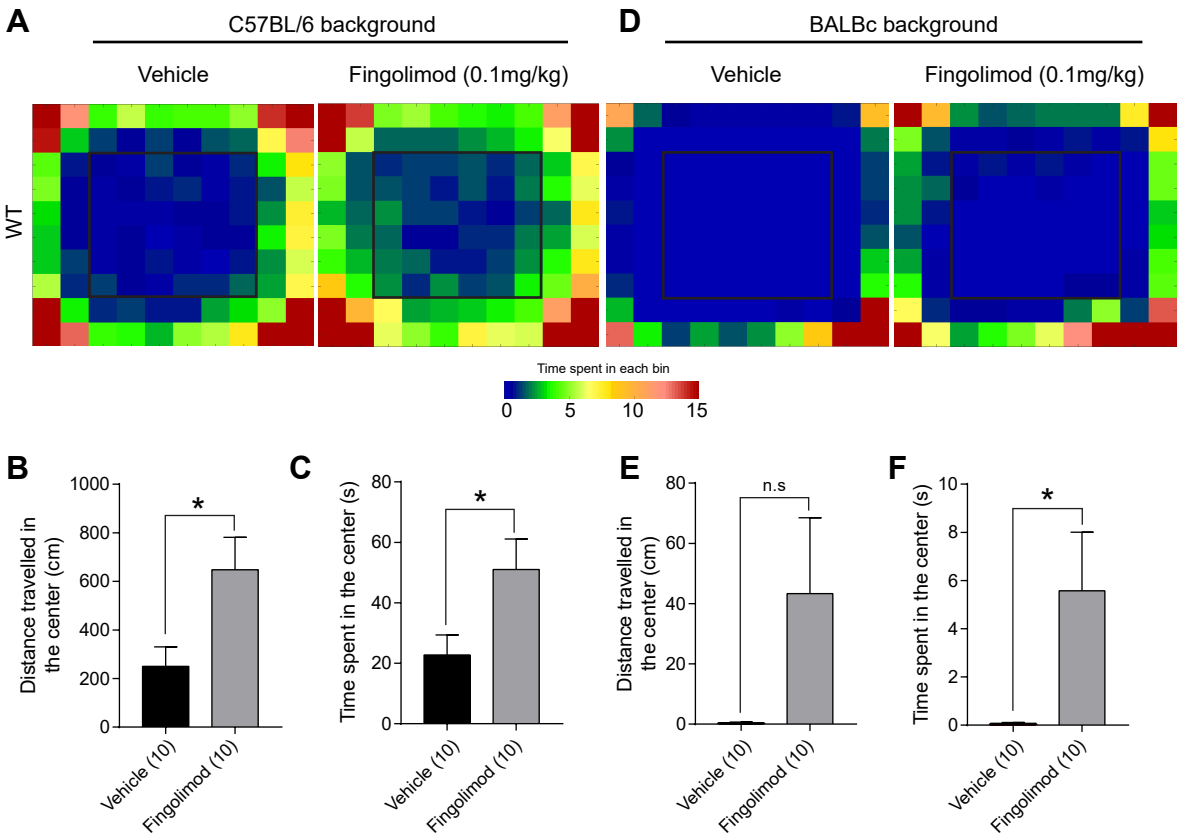
A
C57BL/6 background
Vehicle
Fingolimod (0.1mg/kg)
WT
D
BALBc background
Vehicle
Fingolimod (0.1mg/kg)
Time spent in each bin
0
5
10
15

B
Distance travelled in the center (cm)
1000
800
600
400
200
0
*
Vehicle (10)
Fingolimod (10)
C
Time spent in the center (s)
80
60
40
20
0
*
Vehicle (10)
Fingolimod (10)
E
Distance travelled in the center (cm)
80
60
40
20
0
n.s
Vehicle (10)
Fingolimod (10)
F
Time spent in the center (s)
10
8
6
4
2
0
*
Vehicle (10)
Fingolimod (10)

Fig. S6 (*Related to Fig. 7*)**. Effects of fingolimod in open field tests. A, D**, Density map of mouse exploratory activity in the EPM test showing the effects of fingolimod on wild type C57BL/6 (A) and BALB/c mice (D). **B, C**, Fingolimod has clear and robust anxiolytic effects on C57BL/6 mice, increasing the distance travelled and the time spent in the center of the OF arena. **E, F**, The same experiment in BALB/c mice likewise reveals anxiolytic effects of fingolimod, number of animals per group indicated in parentheses, * $p < 0.05$ (two-tailed t-test (B, C, E, F). All data error bars represent mean +/- SEM.

A. Home-cage locomotion

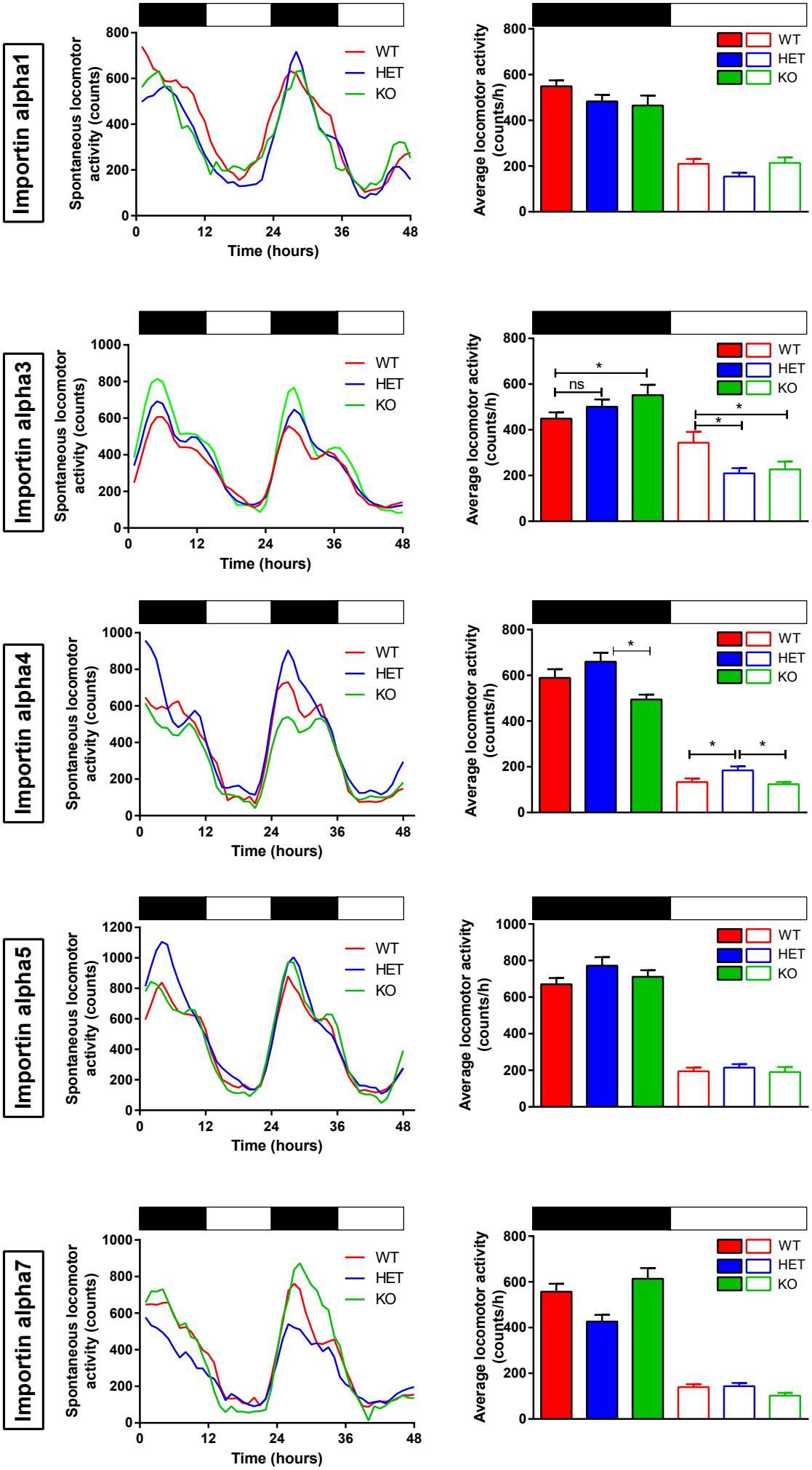

B. Open field test

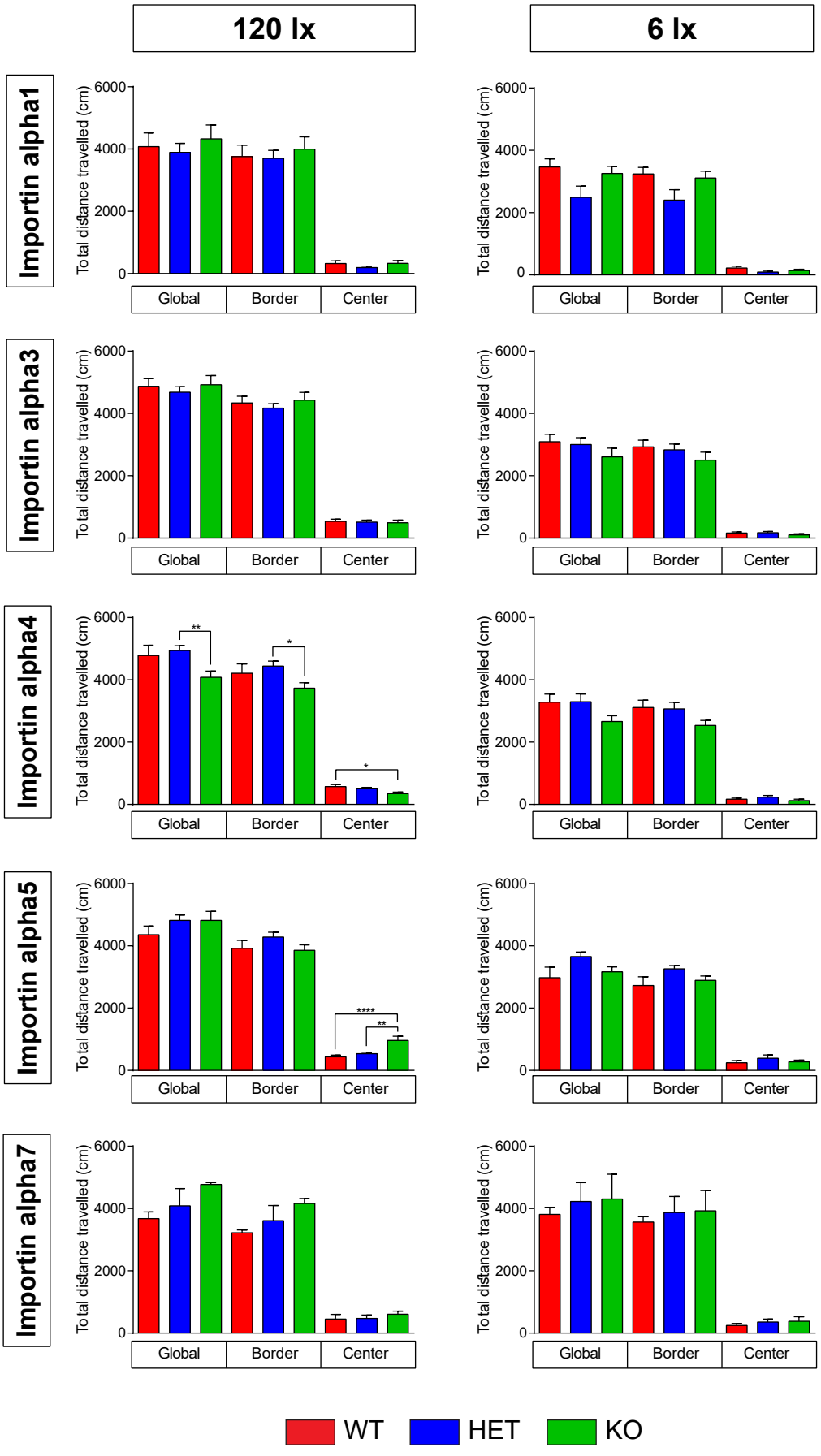

C. Open field test - group heat map

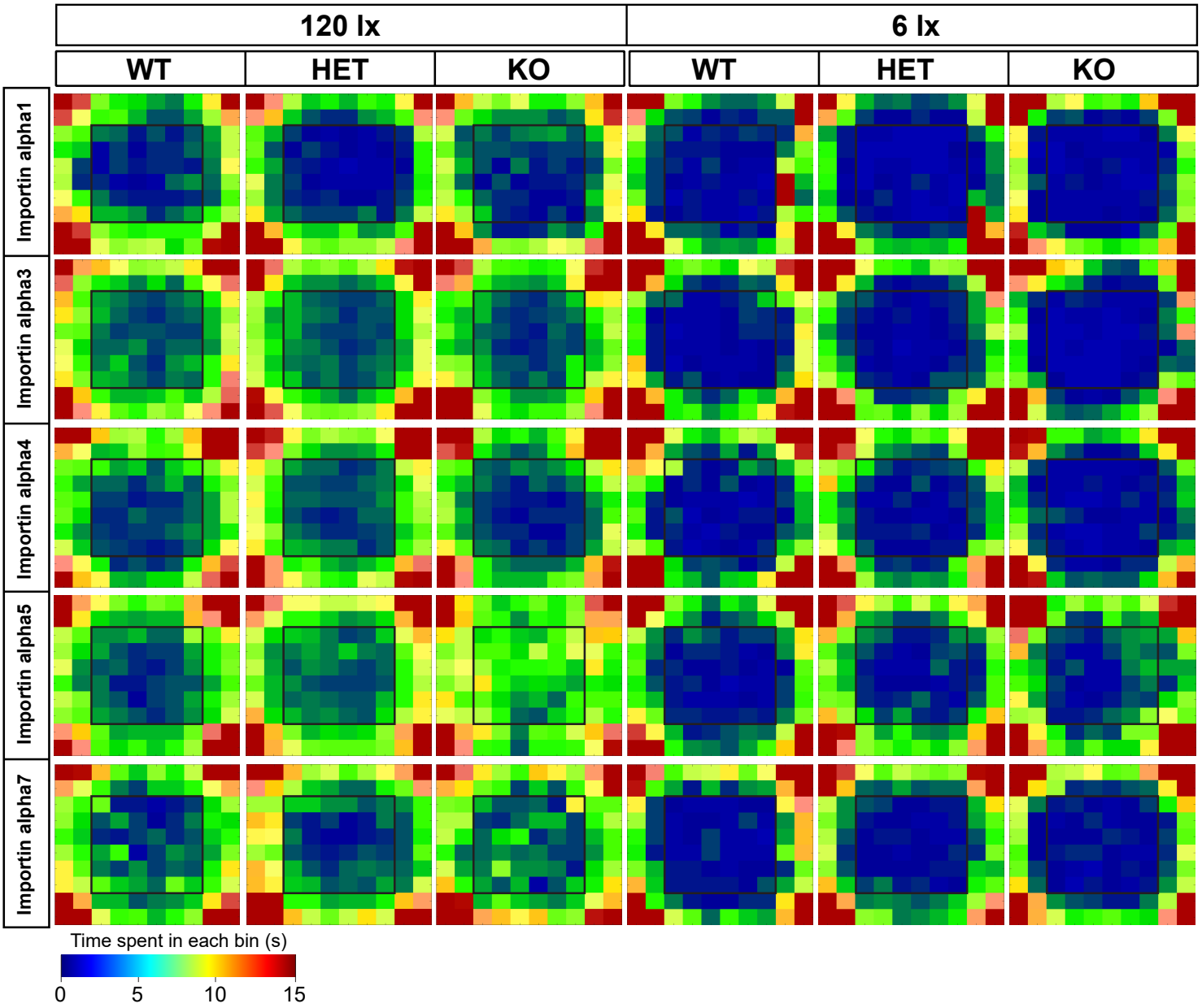

D. Elevated plus maze

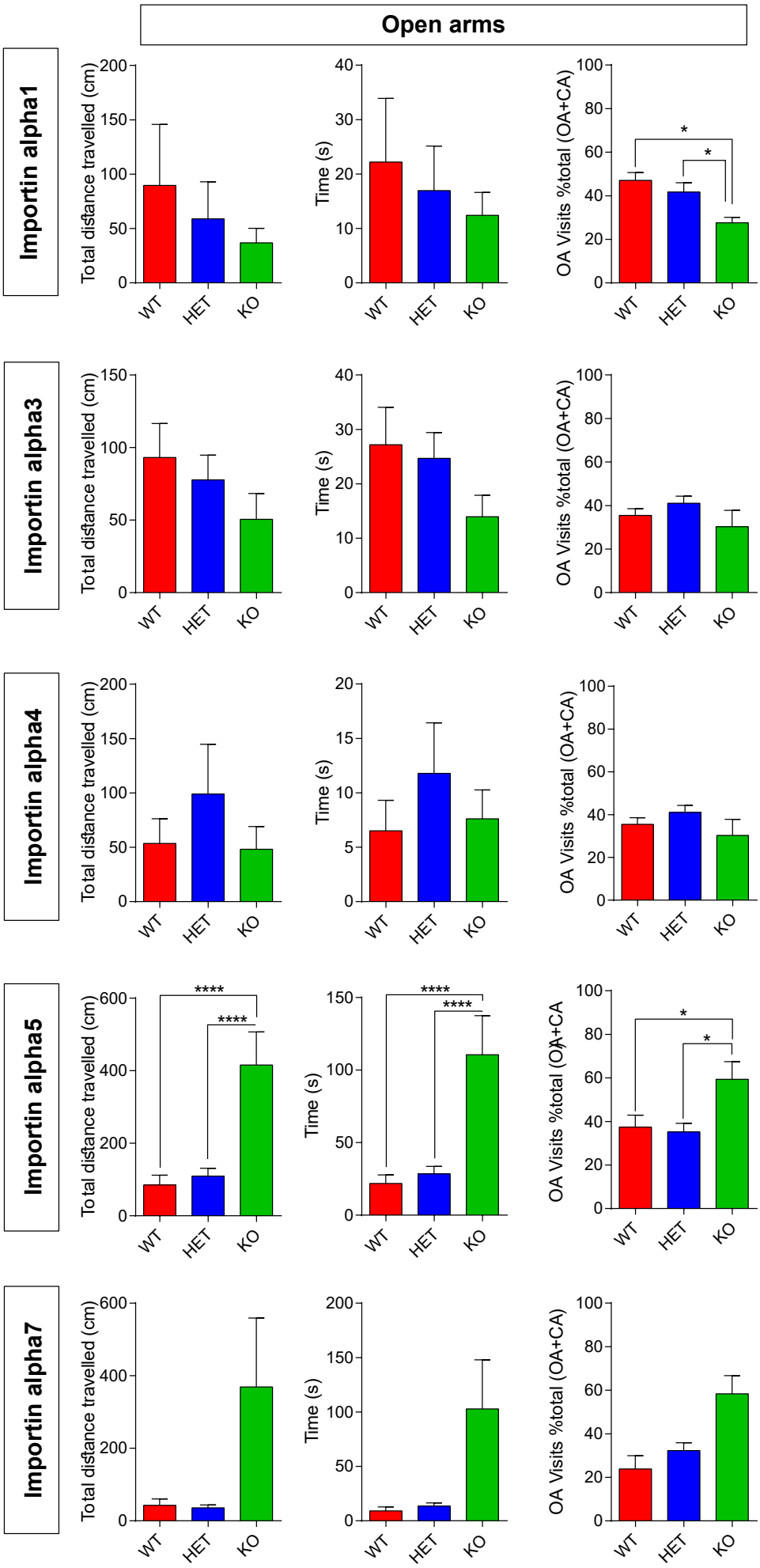

E. Startle response

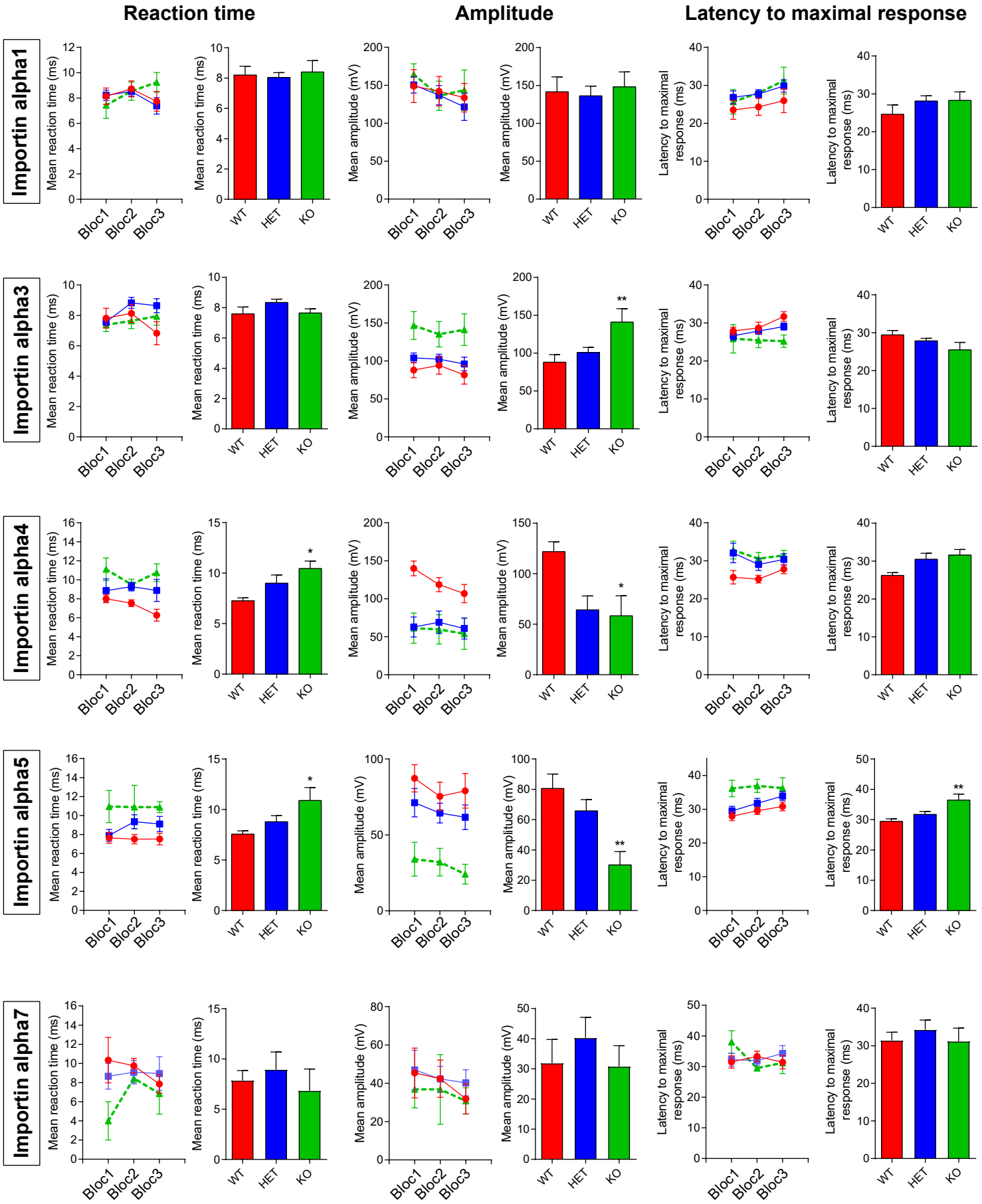

F. Rotarod

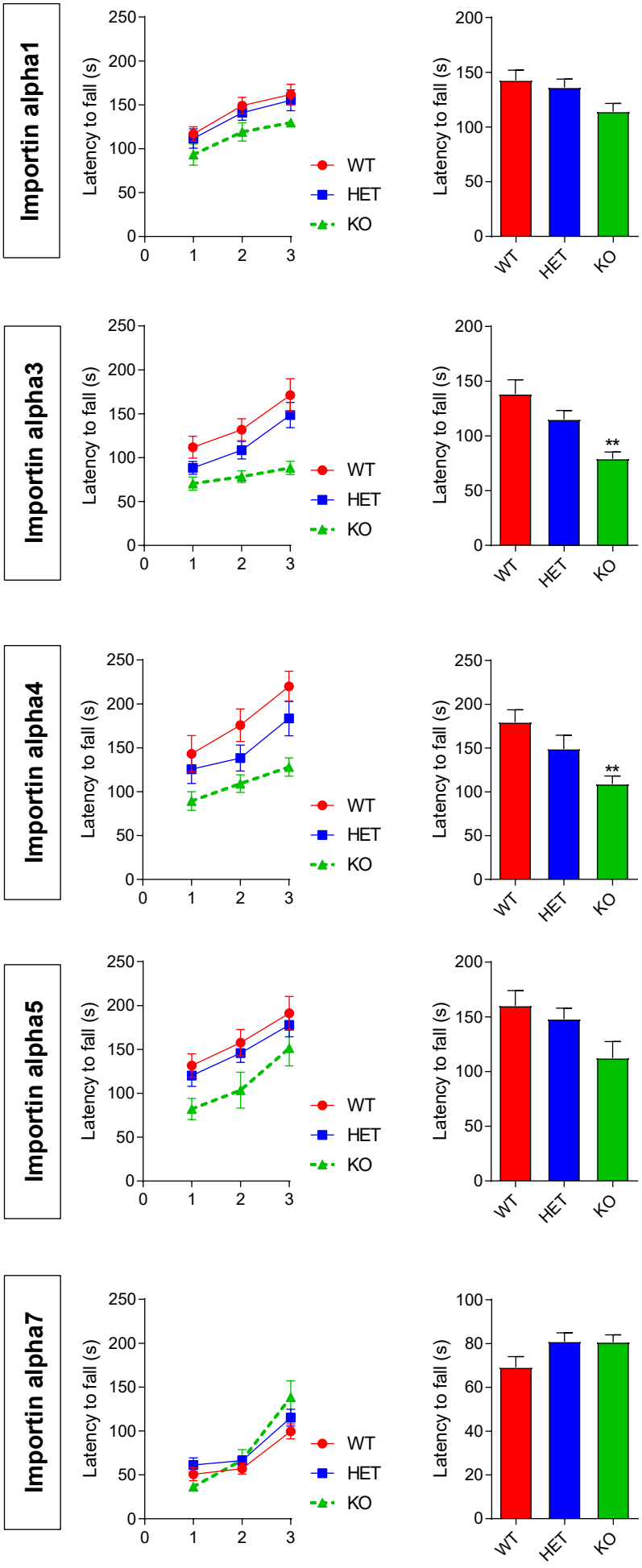
Importin alpha1
Importin alpha3
Importin alpha4
Importin alpha5
Importin alpha7
Latency to fall (s)
WT
HET
KO
**

G. Wire hanging test

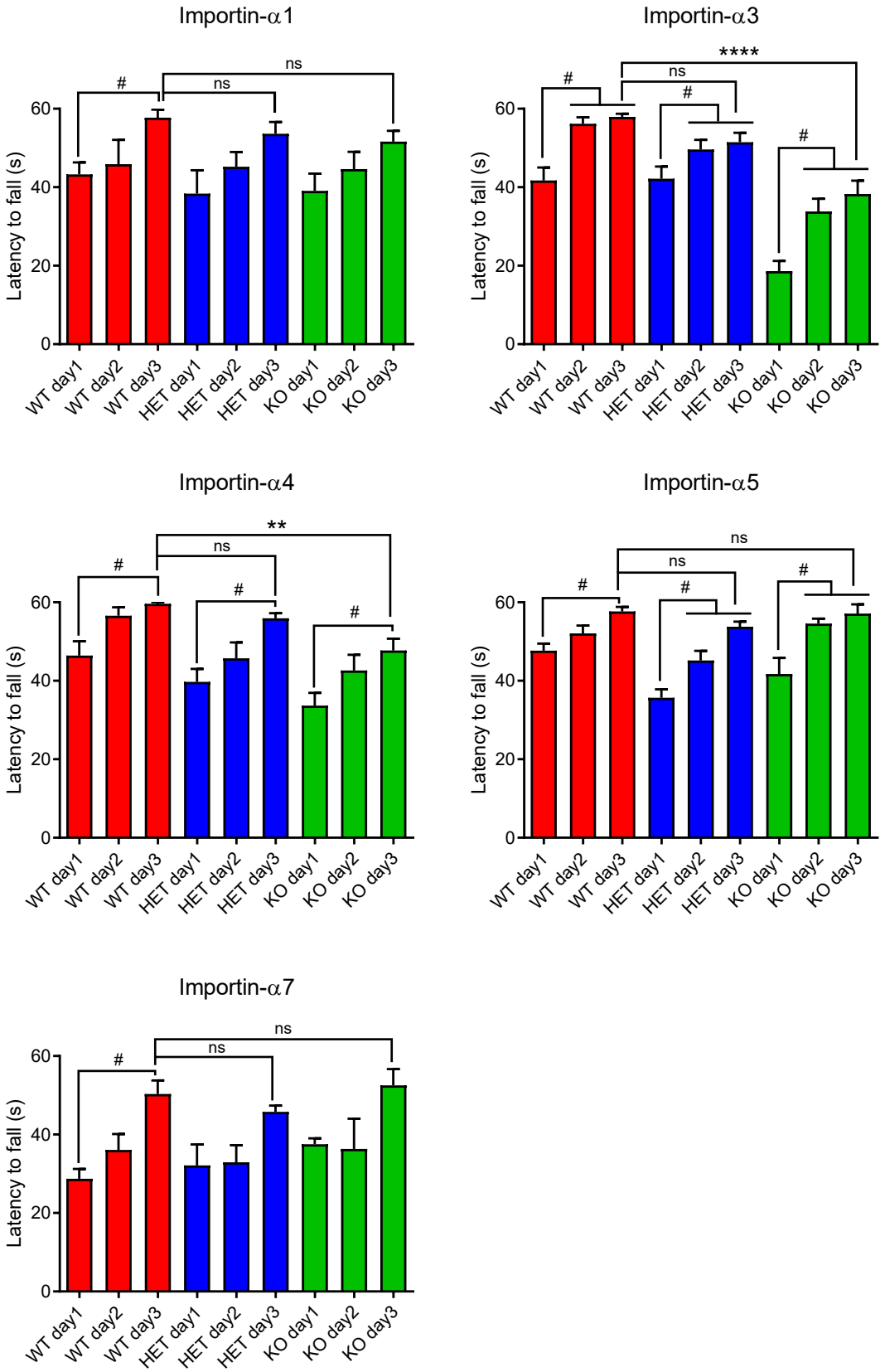

# P<0.05 - RM one-way ANOVA + Sidak's multiple comparisons test
* P<0.05, ** P<0.01, *** P<0.001, **** P<0.0001 - ANOVA + Sidak's multiple comparisons test

H. Pole test

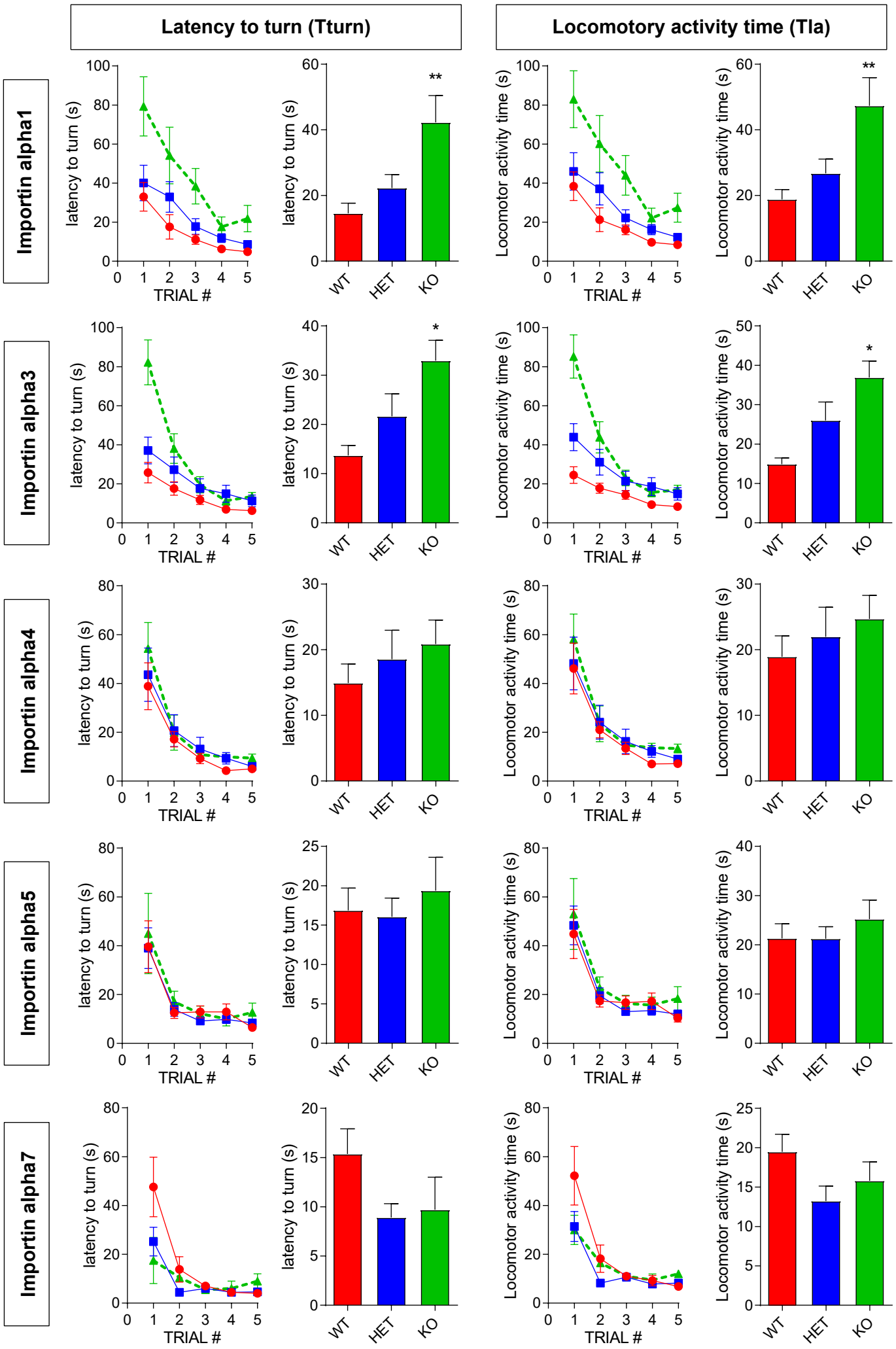
Latency to turn (Tturn)
Locomotory activity time (Tla)
Importin alpha1
Importin alpha3
Importin alpha4
Importin alpha5
Importin alpha7
latency to turn (s)
Locomotor activity time (s)
TRIAL #
WT
HET
KO
**
*

Dataset S1 (*SI related to Fig. 1*)**.** Behavioral profiling of importin α1, α3, α4, α5 and α7 (3 groups per line: wild-type, heterozygous, knockouts). **A**, Home-cage locomotion. Left panel: spontaneous activity along the 48 hrs of the monitoring and the respective average activity in counts/h for the dark (black box) and light periods (white box). **B-C**, Open-field test. Total distance travelled, globally or in the center or border region of the arena under 120lx or 6lx illumination condition (B) and respective open-field group heat-maps of activity (color coding expressed as time spent in each bin) generated with COLORcation (C). **D**, Elevated plus maze. Distance travelled (cm), time spent (s) in the open arms and percentage of open arms visits (OA visits). **E**, Startle response values expressed as reaction time (ms), the amplitude and the latency to produce the maximal response (MaxMs). For each parameter, the left panel depicts the values in each of the 3 blocs while the right panel shows the average responses. **F**, Latency to fall from the accelerating rotarod over the 3 consecutive trials and on average. **G**, Wire-hanging test data expressed as the latency to fall (s). **H**, Pole test latency to turn (Tturn) and locomotory activity time (Tla, time to turn + time needed to reach the cage at the bottom of the vertical pole). 8-15 animals were used for each line in the different assays of this data-set., * $p < 0.05$; ** $p < 0.01$; *** $p < 0.001$, **** $p < 0.0001$ (one-way ANOVA followed by Tukey's HSD post hoc correction for multiple comparisons (A, B, D, E, F, H). Two-way ANOVA showing the intra-group ability to improve the performances from day1 to day3 and one-way ANOVA + Sidak post-hoc analyses to analyze group differences on the last testing day (G).